

Simple yet Effective Graph Distillation via Clustering

Technical Report

Yurui Lai
Hong Kong Baptist University
Hong Kong, China
csylai@comp.hkbu.edu.hk

Taiyan Zhang
ShanghaiTech University
Shanghai, China
zhangty2022@shanghaitech.edu.cn

Renchi Yang
Hong Kong Baptist University
Hong Kong, China
renchi@hkbu.edu.hk

Abstract

Despite plentiful successes achieved by graph representation learning in various domains, the training of *graph neural networks* (GNNs) still remains tenaciously challenging due to the tremendous computational overhead needed for sizable graphs in practice. Recently, *graph data distillation* (GDD), which seeks to distill large graphs into compact and informative ones, has emerged as a promising technique to enable efficient GNN training. However, most existing GDD works rely on heuristics that align model gradients or representation distributions on condensed and original graphs, leading to compromised result quality, expensive training for distilling large graphs, or both. Motivated by this, this paper presents an efficient and effective GDD approach, ClustGDD. Under the hood, ClustGDD resorts to synthesizing the condensed graph and node attributes through fast and theoretically-grounded clustering that minimizes the *within-cluster sum of squares* and maximizes the *homophily* on the original graph. The fundamental idea is inspired by our empirical and theoretical findings unveiling the connection between clustering and empirical condensation quality using *Fréchet Inception Distance*, a well-known quality metric for synthetic images. Furthermore, to mitigate the adverse effects caused by the homophily-based clustering, ClustGDD refines the nodal attributes of the condensed graph with a small augmentation learned via class-aware graph sampling and consistency loss. Our extensive experiments exhibit that GNNs trained over condensed graphs output by ClustGDD consistently achieve superior or comparable performance to state-of-the-art GDD methods in terms of node classification on five benchmark datasets, while being orders of magnitude faster.

CCS Concepts

• **Information systems** → *Clustering*; • **Computing methodologies** → *Supervised learning by classification*; • **Mathematics of computing** → *Graph algorithms*.

Keywords

graph data distillation, graph neural networks, clustering

ACM Reference Format:

Yurui Lai, Taiyan Zhang, and Renchi Yang. 2025. Simple yet Effective Graph Distillation via Clustering: Technical Report. In . ACM, New York, NY, USA, 17 pages. <https://doi.org/XXXXXXX.XXXXXXX>

1 Introduction

In the past decade, *Graph Neural Networks* (GNNs) have emerged as a powerful model for learning on graph-structured data and found extensive practical applications in various fields, including molecular chemistry [22, 46], bioinformatics [11, 42], transportation [5, 23], finance [3, 58], recommendation systems [2, 12, 49], etc. Despite the remarkable success achieved, training GNN models over large-scale graphs with millions of nodes/edges, still remains highly challenging due to the expensive *message passing* operations [17, 60] therein, which demand tremendous computational resources and incur significant time costs [19, 48].

In recent years, inspired by the success of *dataset distillation* [28, 38] in computer vision, a series of *graph data distillation* (GDD, a.k.a., *graph condensation*) [9, 14, 15, 25, 32, 34, 50, 54, 59], techniques have been proposed for expediting GNN training. In particular, GDD aims to distill a compact yet informative graph \mathcal{G}' from the original large graph \mathcal{G} as its surrogate to train the GNN models, such that the models trained on \mathcal{G}' can achieve comparable performance to those on \mathcal{G} . In doing so, we can circumvent the significant expense required for model training on \mathcal{G} and enable efficient inference [13], unlearning [29], graph continual learning [33], hyperparameter search [6], and broader applicability of GNNs.

As reviewed in [15, 51], a major category of existing works focuses on optimizing heuristic objectives that are not directly correlated with the condensation quality, e.g., aligning the model gradients [25, 34, 54], distributions of node representations in each GNN layer [31], long-term training trajectories [33, 59], eigenbasis of graph structures [32], or performance of models (e.g., node classification loss) [44, 53] between the original graph \mathcal{G} and synthetic graph \mathcal{G}' . However, such complex optimizations lead to intensive computations in the course of condensation, rendering them impractical for the distillation of large graphs that pervade the real world. For instance, on the well-known *Reddit* graph with around 233 thousand nodes [18], these approaches [25, 34, 59] consume hours to generate the condensed graph, while the training of GNNs on the entire \mathcal{G} merely takes a few minutes. Recently, several attempts [14, 24, 44] have been made towards enhancing condensation efficiency. Jin et al. [24] propose a one-step scheme to curtail the steps needed for gradient matching, while Wang et al. [44] transform the bi-level optimization architecture for GDD as a *kernel ridge regression* (KRR) task so as to avert iteratively training GNNs. Moreover, Gao et al. [14] introduces a *training-free* GDD framework

Permission to make digital or hard copies of all or part of this work for personal or classroom use is granted without fee provided that copies are not made or distributed for profit or commercial advantage and that copies bear this notice and the full citation on the first page. Copyrights for components of this work owned by others than ACM must be honored. Abstracting with credit is permitted. To copy otherwise, or republish, to post on servers or to redistribute to lists, requires prior specific permission and/or a fee. Request permissions from permissions@acm.org.
KDD'25, Toronto, ON, Canada

© 2025 ACM.
ACM ISBN 978-1-4503-XXXX-X/18/06
<https://doi.org/XXXXXXX.XXXXXXX>

that reduces the costly node distribution matching to a tractable class partition problem. Unfortunately, these methods trade effectiveness for higher efficiency, and hence, produce compromised condensation quality.

To overcome the aforementioned deficiencies, this paper presents ClustGDD (Clustering-based Graph Data Distillation), an effective and efficient solution for GDD via two simple steps: *clustering* and *attribute refinement*. ClustGDD takes inspiration from our empirical observation that *Fréchet Inception Distance* (FID) [8], a prominent metric for measuring the quality of synthetic images created by generative models with real images, can also accurately evaluate the condensation quality (i.e., node classification performance of GNNs) of real graphs without ground-truth node labels. In particular, on a condensed graph \mathcal{G}' with a low FID, GNN models trained on \mathcal{G}' always yield a high prediction accuracy in node classification, as illustrated in Fig. 1. Our theoretical analysis further unveils that mapping node clusters of \mathcal{G} with the minimum *within-cluster sum of squares* (WCSS) of node representations as synthetic nodes can generate \mathcal{G}' with a bounded and optimized FID. This motivates us to construct condensed graphs with high quality through proper clustering of nodes in \mathcal{G} .

Specifically, we first develop a clustering method in ClustGDD that seeks to minimize the WCSS of node representations, which can be framed as a standard K -Means task. As such, the key then lies in the construction of node representations, such that nodes in \mathcal{G} with the same ground-truth class labels are close, whereas those in distinct classes are distant. Doing so facilitates not only the minimization of the WCSS via K -Means clustering for a lower FID, but also the accurate classification of the corresponding nodes. Using the *homophily assumption* [61] for graphs, ClustGDD generates the above-mentioned node embeddings for clustering by optimizing the *graph Laplacian smoothing* (GLS) [7] and training a linear layer with label supervision. Based thereon, condensed graph topology, synthetic node attributes, and labels, can be easily derived. On top of that, in order to mitigate the *heterophilic over-smoothing issue* caused by this homophily-based clustering, ClustGDD additionally includes a lightweight module CAAR (Class-Aware Attribute Refinement). More concretely, CAAR refines the synthetic node attributes by injecting class-relevant features learned on class-specific graphs from \mathcal{G}' using our carefully-designed sampling technique. Such a small augmentation enlarges the attribute distance of heterophilic nodes (i.e., nodes with distinct class labels), thereby effectively alleviating the over-smoothing problem in node representations.

In summary, our contributions in this paper are as follows:

- We are the first to extend the FID for image data to assess the GDD quality and validate its empirical effectiveness. We establish the theoretical connection between clustering and FID optimization, which inspires the design of effective GDD.
- Methodologically, we propose ClustGDD, an effective and efficient GDD solution that leverages a simple clustering approach aiming at optimizing the WCSS and homophily for graph synthesis, followed by a module CAAR focusing on a slight refinement of the synthetic node attributes.
- Empirically, we conduct extensive experiments on multiple benchmark datasets to demonstrate the superior condensation effectiveness and efficiency of ClustGDD over existing GDD methods.

2 Preliminaries

2.1 Symbols and Terminology

Let $\mathcal{G} = (\mathcal{V}, \mathcal{E}, X)$ be an attributed graph, where \mathcal{V} is a set of $N = |\mathcal{V}|$ nodes, \mathcal{E} is a set of $M = |\mathcal{E}|$ edges, and $X \in \mathbb{R}^{N \times d}$ symbolizes the node attribute matrix. For each edge $e_{i,j} \in \mathcal{E}$, we say v_i and v_j are neighbors to each other and use $\mathcal{N}(v_i)$ to denote the set of neighbors of v_i , whose degree is $d(v_i) = |\mathcal{N}(v_i)|$. Each node $v_i \in \mathcal{V}$ is associated with a d -dimensional attribute vector X_i . The adjacency matrix of \mathcal{G} is denoted as $A \in \{0, 1\}^{N \times N}$, wherein $A_{i,j} = A_{j,i} = 1$ if $(v_i, v_j) \in \mathcal{E}$, and 0 otherwise. The degree matrix of \mathcal{G} is represented by D , whose i -th diagonal entry $D_{i,i} := d(v_i)$. Accordingly, the normalized adjacency matrix of \mathcal{G} is represented by $\tilde{A} = D^{-1/2} A D^{-1/2}$ and $I - \tilde{A}$ is known as its graph Laplacian. We use $\text{tr}(\cdot)$ to denote the trace of a matrix.

Homophily Ratio. Given a set of K classes \mathcal{Y} ($K := |\mathcal{Y}|$) and the class label $y_i \in \mathcal{Y}$ for each node $v_i \in \mathcal{V}$, the *homophily ratio* [61] of \mathcal{G} is calculated by $\Omega(\mathcal{G}) = \frac{|\{(v_i, v_j) \in \mathcal{E} : y_i = y_j\}|}{m}$, which quantifies the fraction of homophilic edges that connect nodes of the same classes [61]. The label matrix of \mathcal{G} is denoted as $Y \in \{0, 1\}^{N \times K}$, wherein $Y_{i,j} = 1$ if $y_i = j$ and 0 otherwise.

Fréchet Inception Distance. *Fréchet Inception Distance* (FID) [8] is originally used to measure the discrepancy between two multivariate normal distributions and is later adopted as the standard metric for assessing the quality of synthetic images from generative models [20]. Let μ^{org} and μ^{syn} be the mean of the Inception embeddings of real and synthetic images, respectively, and Σ^{org} , Σ^{syn} be their respective covariances between features. The FID is expressed in closed form as

$$\text{FID} = \|\mu^{\text{org}} - \mu^{\text{syn}}\|_2^2 + \text{tr} \left(\Sigma^{\text{org}} + \Sigma^{\text{syn}} - 2(\Sigma^{\text{org}} \Sigma^{\text{syn}})^{\frac{1}{2}} \right), \quad (1)$$

where the first term calculates the average distance between two embedding spaces to represent the overall distribution shift, while the second term involves the trace of the covariance matrices and the geometric mean of the covariance matrices, measuring the difference in the shape and spread of the feature distributions of original and synthetic graphs. A lower FID value indicates better synthetic quality, and the generative model is perfect when $\Phi = 0$.

Graph Laplacian Smoothing. Given graph \mathcal{G} , *graph Laplacian smoothing* (GLS) [7] is to optimize Z such that

$$\min_Z (1 - \alpha) \cdot \|Z - X\|_F^2 + \alpha \sum_{(v_i, v_j) \in \mathcal{E}} \left\| \frac{Z_i}{\sqrt{d(v_i)}} - \frac{Z_j}{\sqrt{d(v_j)}} \right\|_F^2. \quad (2)$$

Therein, the fitting term $\|Z - X\|_F^2$ in Eq. (2) seeks to make the node features Z close to the initial attributes X , while the graph Laplacian regularization term $\sum_{(v_i, v_j) \in \mathcal{E}} \left\| \frac{Z_i}{\sqrt{d(v_i)}} - \frac{Z_j}{\sqrt{d(v_j)}} \right\|_F^2$ forces feature vectors of two adjacent nodes in \mathcal{G} to be similar. The hyperparameter $\alpha \in [0, 1]$ controls the smoothness of Z over \mathcal{G} . As revealed in recent studies [37, 62], after removing non-linear operations and linear transformations, graph convolutional operations in most GNN models [4, 16, 26, 52] essentially are to optimize the GLS objective in Eq. (2).

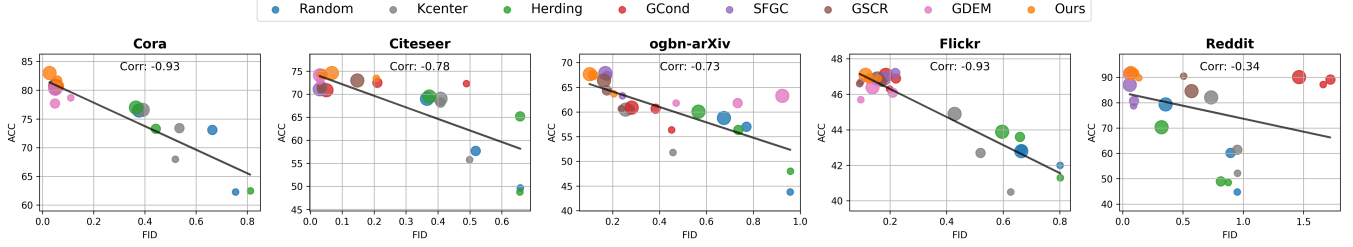


Figure 1: Classification accuracy v.s. FID under various condensation ratios.

2.2 Graph Data Distillation (GDD)

Given an input graph $\mathcal{G} = (\mathcal{V}, \mathcal{E}, X)$, GDD is to distill from \mathcal{G} a condensed graph \mathcal{G}' with a set $V' = \{u_1, u_2, \dots, u_n\}$ of n ($n \ll N$) nodes, a set \mathcal{E}' of m ($m \ll M$) edges, and synthetic attribute vectors $X' \in \mathbb{R}^{n \times d}$ for n nodes, and the adjacent matrix $A' \in \{0, 1\}^{n \times n}$. Each node $u_i \in \mathcal{G}'$ is associated with a synthetic class label $y_i \in \mathcal{Y}$ and the label matrix of \mathcal{G}' is symbolized by $Y' \in \mathbb{R}^{n \times K}$. In the meantime, GNNs trained on the condensed graph \mathcal{G}' should achieve comparable performance to those on the original graph \mathcal{G} . Let $\mathcal{L}(\cdot, \cdot)$ be an inaccuracy metric for node classification tasks. In mathematical terms, the optimization goal of GDD can be formulated as follows [34]:

$$\begin{aligned} \min \quad & \mathcal{L}(\text{GNN}_{\Theta_{\mathcal{G}'}}(A', X'), Y') \\ \text{s.t.} \quad & \Theta_{\mathcal{G}'} = \arg \min_{\Theta} \mathcal{L}(\text{GNN}_{\Theta}(A', X'), Y'), \end{aligned}$$

where $\text{GNN}_{\Theta}(\cdot)$ denotes a GNN model parameterized with Θ and $\Theta_{\mathcal{G}'}$ are the model parameters obtained via training the GNN over the condensed graph \mathcal{G}' . To get detailed information of representative types of GDD, please check Appendix A.

3 Condensation Quality Analysis

In this section, we first extend FID to assess the quality of condensed graphs by GDD methods and validate its empirical effectiveness on real datasets. Next, we conduct a theoretical analysis of FID to pinpoint a design principle for effective GDD.

3.1 FID as Condensation Quality Metric

Given the original graph \mathcal{G} and the condensed graph \mathcal{G}' , we propose to evaluate the condensation quality of \mathcal{G}' via the FID of node representations H and H' learned by GNNs (e.g., GCN) over \mathcal{G} and \mathcal{G}' . Specifically, we define

$$\mu^{\text{org}} = \frac{1}{N} \sum_{v_i \in \mathcal{G}} H_i \text{ and } \mu^{\text{syn}} = \frac{1}{n} \sum_{u_i \in \mathcal{G}'} H'_i. \quad (3)$$

Let \hat{H} and \hat{H}' represent the centered versions of H and H' , respectively. The covariance matrices Σ^{org} and Σ^{syn} of H and H' then can be formulated as

$$\Sigma^{\text{org}} = \frac{1}{N} \hat{H}^T \hat{H} \text{ and } \Sigma^{\text{syn}} = \frac{1}{n} \hat{H}'^T \hat{H}'. \quad (4)$$

The FID of H and H' can thus be computed as per Eq. (1).

Accordingly, the first term $\|\mu^{\text{org}} - \mu^{\text{syn}}\|_2^2$ in the FID quantifies the dissimilarity of these two node representations, reflecting how much on average the condensed graph \mathcal{G}' resembles \mathcal{G} and captures the key structural and attribute characteristics therein. On the other

hand, recall that a larger covariance value in Σ^{org} or Σ^{syn} indicates a wider spread of feature values, while off-diagonal elements represent correlations between different feature dimensions. The second term $\text{Tr}(\Sigma^{\text{org}} + \Sigma^{\text{syn}} - 2(\Sigma^{\text{org}} \Sigma^{\text{syn}})^{\frac{1}{2}})$ is thus the difference in the spread of individual feature dimensions of H and H' and correlations between them, measuring how different the “shape” of the feature distributions underlying \mathcal{G} and \mathcal{G}' are. Intuitively, a lower FID connotes a closer match between these two data distributions, and hence, a higher condensation quality of H' .

Empirical Study. To verify the empirical effectiveness of FID in measuring the condensation quality, we experimentally evaluate the GNN performance on the condensed graphs \mathcal{G}' obtained via various GDD approaches over real graph datasets in downstream tasks (i.e., node classification) and their corresponding FID values.¹ Fig. 1 plots the classification accuracies and FID scores of the Random [47], Kcenter [41], and Herding [47] coreset methods, as well as GDD approaches including GCond [25], SFGC [59], CSCR [34], GDEM [32], and our proposed ClustGDD on *Citeseer*, *Cora*, *arXiv*, and *Flickr*. Each method is represented by three bubbles, which correspond to their results under three different condensation ratios commonly used in previous works [25]. It can be observed from Fig. 1 that in almost all cases, a method with a low FID will yield high accuracy in the downstream node classification tasks, implying a linear correlation between the FID of \mathcal{G}' and the GNN model performance over it. In turn, FID can serve as a precise quality metric for condensed graphs practically, even without ground-truth labels.

3.2 Theoretical Inspiration

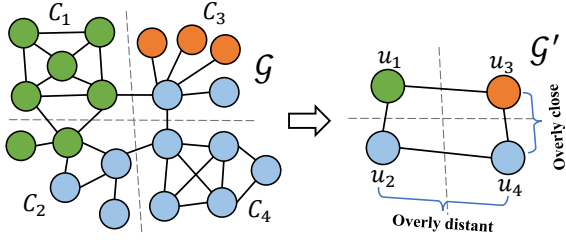
Ideally, a high-quality condensed graph \mathcal{G}' should minimize the first term $\|\mu^{\text{org}} - \mu^{\text{syn}}\|_2^2$ in the FID, meaning that

$$\sum_{u_i \in \mathcal{G}'} H'_i \approx \sum_{v_i \in \mathcal{G}} \frac{n}{N} \cdot H_i.$$

Intuitively, the minimization can be attained when the representation H'_i of each node $u_i \in \mathcal{G}'$ is a weighted summation of the representations of a subset C_i of nodes in \mathcal{G} , i.e., $H'_i = \sum_{v_j \in C_i} w_j \cdot H_j$, such that $\bigcup_{i=1}^n C_i = \mathcal{V}$ and $C_i \cap C_j = \emptyset \forall i \neq j, 1 \leq i, j \leq n$. As such, each node u_i in \mathcal{G}' is a supernode merged from the nodes inside a cluster C_i . Along this line, a simple and straightforward approach to constructing the condensed graph \mathcal{G}' is to partition the input graph \mathcal{G} into n disjoint clusters $\{C_1, \dots, C_n\}$.

$$\text{THEOREM 3.1. } \|\mu^{\text{org}} - \mu^{\text{syn}}\|_2^2 \leq \frac{1}{N^2} \sum_{i=1}^n \left(\frac{N}{n} - |C_i| \right)^2.$$

¹In practice, we normalize the representations to control the range of FID values.

Figure 2: Example of a balanced clustering of \mathcal{G} .

When we let u_i 's representation be the averaged embeddings of the nodes inside cluster C_i , i.e., $H'_i = \sum_{v_j \in C_i} \frac{H_j}{|C_i|}$, our Theorem 3.1 reveals that the first term $\|\mu^{\text{org}} - \mu^{\text{syn}}\|_2^2$ in the FID can be bounded by $\frac{1}{N^2} \sum_{i=1}^n \left(\frac{N}{n} - |C_i| \right)^2$. Since $\sum_{i=1}^n |C_i| = N$, the mean cluster size is thus $\frac{N}{n}$. This upper bound is essentially the *variance* of the sizes of n clusters $\{C_1, \dots, C_n\}$ scaled by $\frac{1}{N}$. In particular, $\|\mu^{\text{org}} - \mu^{\text{syn}}\|_2^2$ is minimized, i.e., $\|\mu^{\text{org}} - \mu^{\text{syn}}\|_2^2 \approx 0$, when the size of every cluster C_i is approximately $\frac{N}{n}$.

THEOREM 3.2. Let $c_{\max} = \max_{1 \leq i \leq n} |C_i|$ and $c_{\min} = \min_{1 \leq i \leq n} |C_i|$. Then, $\text{Tr}(\Sigma^{\text{org}} + \Sigma^{\text{syn}} - 2(\Sigma^{\text{org}} \Sigma^{\text{syn}})^{\frac{1}{2}}) \leq \frac{1}{N} \sum_{i=1}^n \sum_{v_j \in C_i} \|H_j - H'_i\|_2^2 + \frac{nc_{\max}}{N} \cdot \|\mu^{\text{org}} - \mu^{\text{syn}}\|_2^2 + \left(\frac{c_{\max}}{c_{\min}} + \frac{N}{nc_{\min}} \right) \cdot \text{Tr}(\Sigma^{\text{org}})$ holds.

As for the second term $\text{Tr}(\Sigma^{\text{org}} + \Sigma^{\text{syn}} - 2(\Sigma^{\text{org}} \Sigma^{\text{syn}})^{\frac{1}{2}})$ in the FID, Theorem 3.2 states that its upper bound is positively correlated with $\frac{1}{N} \sum_{i=1}^n \sum_{v_j \in C_i} \|H_j - H'_i\|_2^2$, the first term in FID (i.e., $\|\mu^{\text{org}} - \mu^{\text{syn}}\|_2^2$), and $\text{Tr}(\Sigma^{\text{org}})$. Notice that $\|\mu^{\text{org}} - \mu^{\text{syn}}\|_2^2$ can be bounded by Theorem 3.1, and $\text{Tr}(\Sigma^{\text{org}})$ is solely determined by the input graph \mathcal{G} , and hence, can be regarded as a constant. Therefore, we can reduce the second term $\text{Tr}(\Sigma^{\text{org}} + \Sigma^{\text{syn}} - 2(\Sigma^{\text{org}} \Sigma^{\text{syn}})^{\frac{1}{2}})$ and further the FID, by minimizing $\frac{1}{N} \sum_{i=1}^n \sum_{v_j \in C_i} \|H_j - H'_i\|_2^2$, which is essentially the WCSS, i.e., the variance of feature representations within each cluster.

In a nutshell, the foregoing analyses suggest a promising way to construct the condensed graph \mathcal{G}' with a bounded and low FID through partitioning the original node set \mathcal{V} of \mathcal{G} into clusters, particularly with balanced sizes and small WCSS, as the n synthetic nodes in \mathcal{G}' . For the proofs of the theorems, please refer to the Appendix E for details.

4 Methodology

In this section, we present ClustGDD for distilling \mathcal{G} as \mathcal{G}' . We first elaborate on our clustering method for creating the condensed graph structure A' , synthetic attribute matrix X' , and node labels Y' in Section 4.1. In Section 4.2, we further pinpoint the defects of X' generated by the clustering and delineate a class-aware scheme CAAR for refining X' . To facilitate a better comprehension of ClustGDD, we present its overall framework in Fig. 3.

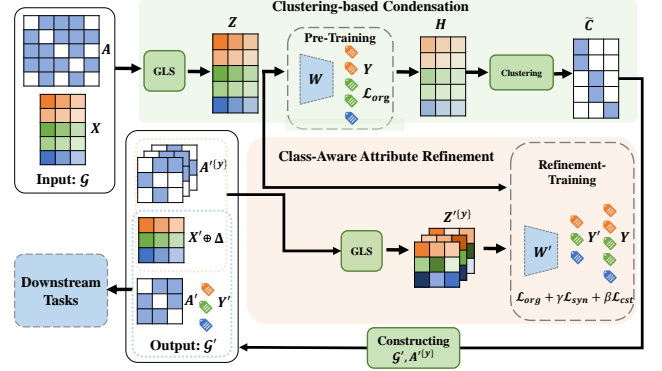


Figure 3: An overview of ClustGDD.

4.1 Clustering-based Condensation

Let $\{C_1, \dots, C_n\}$ be a partition of n clusters of \mathcal{G} and each synthetic node u_i in \mathcal{G}' be merged from the cluster C_i , i.e.,

$$H'_i = \sum_{v_j \in C_i} \frac{H_j}{|C_i|} \quad (5)$$

According to our analysis in Section 3.2, a low FID between \mathcal{G} and \mathcal{G}' can be obtained with clusters $\{C_1, \dots, C_n\}$ that optimize

$$\min_{C_1, C_2, \dots, C_n} \sum_{i=1}^n \sum_{v_j \in C_i} \|H_j - H'_i\|_2^2 \quad (6)$$

and meanwhile minimize the cluster size variance $\sum_{i=1}^n \left(\frac{N}{n} - |C_i| \right)^2$. However, the latter optimization objective is likely to group nodes with various class labels into C_i (i.e., the synthetic node u_i) when the ground-truth classes in \mathcal{G} are imbalanced, which is often the case in practice. As exemplified in Fig. 2, this will render some synthetic nodes with distinct synthetic class labels in \mathcal{G}' overly distant (e.g., u_2 and u_4) or close (e.g., u_3 and u_4), and thus, result in degraded condensation quality. Instead, an ideal cluster C_i (i.e., synthetic node u_i) should comprise original nodes associated with the same ground-truth label, which requires the representations of nodes within C_i or the same ground-truth class to be highly similar. By generating such node representations, each term $\sum_{v_j \in C_i} \|H_j - H'_i\|_2^2$ in our objective in Eq.(6) can be implicitly minimized.

Clustering via Optimizing the WCSS and Homophily. Given node representations H of \mathcal{G} , the minimization of the WCSS in Eq.(6) can be efficiently solved using K -Means algorithm [35]. Next, we elucidate the construction of H and how we can enforce nodes with the same class labels to be close in H .

LEMMA 4.1. The closed-form solution to the GLS optimization problem in Eq. (2) is $\sum_{t=0}^{\infty} (1 - \alpha) \alpha^t \tilde{A}^t X$.

As pinpointed in Section 2.1, the representation learning in most GNNs can be unified into a framework optimizing the GLS problem in Eq. (2) or its variants. As per the result in Lemma 4.1, we then construct H by Eq. (7) as Z is the closed-form solution to Eq. (2) when $T \rightarrow \infty$.

$$H = ZW \text{ where } Z = \sum_{t=0}^T (1 - \alpha) \alpha^t \tilde{A}^t X. \quad (7)$$

Particularly, the weights $\mathbf{W} \in \mathbb{R}^{d \times K}$ are learned by minimizing the following cross-entropy loss:

$$\mathcal{L}_{org} = -\frac{1}{N} \sum_{i=1}^N \sum_{y=1}^K Y_{i,y} \cdot \log(P_{i,y}) \quad (8)$$

with the label predictions $\mathbf{P} \in \mathbb{R}^{N \times K}$ transformed from \mathbf{H} via

$$\mathbf{P} = \text{Softmax}(\mathbf{H}), \quad (9)$$

and ground-truth labels for the training set in a supervised fashion

$$\text{LEMMA 4.2. } \Omega(\mathcal{G}) = 1 - \frac{1}{2M} \cdot \sum_{(v_i, v_j) \in \mathcal{E}} \left\| \frac{(D^{1/2} \mathbf{Y})_i}{\sqrt{d_i}} - \frac{(D^{1/2} \mathbf{Y})_j}{\sqrt{d_j}} \right\|_2^2.$$

If we regard \mathbf{H} as the label predictions, our Lemma 4.2 implies that the second term $\sum_{(v_i, v_j) \in \mathcal{E}} \left\| \frac{\mathbf{H}_i}{\sqrt{d(v_i)}} - \frac{\mathbf{H}_j}{\sqrt{d(v_j)}} \right\|_F^2$ in GLS (Eq. (2)) is essentially equivalent to maximizing the homophily ratio of the predicted labels over the input graph \mathcal{G} , whose true homophily ratio is usually assumed to be high in practice, i.e., adjacent nodes are very likely to share the same class labels. Based on this homophily assumption, our way of computing \mathbf{H} in Eq. (7) tends to render the representations of nodes with the same class labels close to each other and easier to be grouped into the same clusters by the K -Means, thereby minimizing the WCSS in Eq. (6).

Constructing \mathbf{X}' , \mathbf{A}' , and \mathbf{Y}' . Denote by $\mathbf{C} \in \{0, 1\}^{N \times n}$ the node-cluster membership matrix, where $C_{j,i} = 1$ if node $v_j \in C_i$ and 0 otherwise. Accordingly, we can form a sketching matrix $\tilde{\mathbf{C}}$ by normalizing \mathbf{C} : $\tilde{\mathbf{C}} = \mathbf{C} \text{diag}(\mathbf{1}\mathbf{C})^{-1}$, where $\tilde{C}_{j,i} = \frac{1}{|C_i|}$ if node $v_j \in C_i$ and 0 otherwise. By Eq. (5), $\mathbf{H}' = \tilde{\mathbf{C}}^\top \mathbf{H}$.

Intuitively, \mathbf{H}' should be built from the condensed adjacency matrix \mathbf{A}' and attribute matrix \mathbf{X}' using Eq. (7). Along this line, we can formulate the following objective function:

$$\min_{\mathbf{A}', \mathbf{X}'} \left\| \tilde{\mathbf{C}}^\top \mathbf{H} - \sum_{t=0}^{T'} (1 - \alpha') \alpha'^t \mathbf{A}'^t \mathbf{X}' \mathbf{W}' \right\|_F^2, \quad (10)$$

where hyperparameters T' , α' , and weights \mathbf{W}' can be configured or learned accordingly in the GNN model trained on \mathcal{G}' . Due to the scale and complexity of the input graph structures, synthesizing the \mathbf{A}' such that $\sum_{t=0}^{T'} (1 - \alpha') \alpha'^t \mathbf{A}'^t$ is close to $\tilde{\mathbf{C}} \sum_{t=0}^T (1 - \alpha) \alpha^t \tilde{\mathbf{A}}^t$ is highly challenging and usually engenders substantial structural information loss. As a workaround, we turn to incorporate most features in \mathbf{H} into \mathbf{X}' as follows:

$$\mathbf{X}' = \tilde{\mathbf{C}}^\top \mathbf{Z} \quad (11)$$

and compress $\tilde{\mathbf{A}}$ as \mathbf{A}' using $\mathbf{A}' = \tilde{\mathbf{C}}^\top \tilde{\mathbf{A}} \tilde{\mathbf{C}}$. Additionally, the synthetic label for each node $u_i \in \mathcal{G}'$ is constructed by

$$Y'_{i,j} = \begin{cases} 1, & \text{if } j = \arg \max_{1 \leq \ell \leq K} H'_{i,\ell}; \\ 0, & \text{otherwise.} \end{cases}$$

4.2 Class-Aware Attribute Refinement (CAAR)

Heterophilic Over-smoothing Issue. Although the clustering approach in the preceding section can produce high-quality condensed graphs, it strongly relies on the homophily assumption.

Table 1: The homophilic ratio $\Omega(\mathcal{G})$ and ICAD of \mathbf{X} , \mathbf{X}' , and $\mathbf{X}' + \beta \cdot \Delta$ on real-world graph datasets.

Dataset	Cora	Citeseer	arXiv	Reddit
$\Omega(\mathcal{G})$	0.81	0.74	0.66	0.78
$\phi(\mathbf{X}, \mathbf{Y})$	0.95	0.96	0.99	0.99
$\phi(\mathbf{X}', \mathbf{Y}')$	0.56	0.51	0.97	0.82
$\phi(\mathbf{X}' + \beta \cdot \Delta, \mathbf{Y}')$	0.77	0.56	1.00	0.96

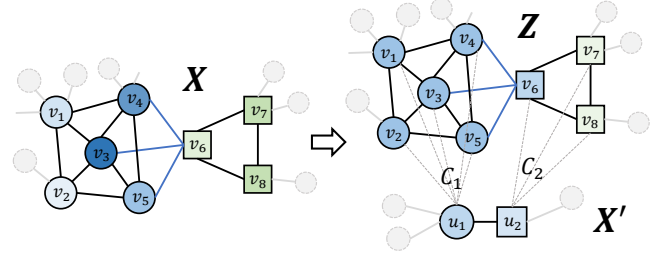


Figure 4: Example of the heterophilic over-smoothing issue

However, according to the homophily ratios of real graphs in Table 1, even in *homophilic graphs*, we can observe a small moiety of *heterophilic links*, i.e., adjacent nodes with distinct ground-truth labels. Recall that \mathbf{Z} in \mathbf{X}' computed via Eq. (11) is to minimize $\sum_{(v_i, v_j) \in \mathcal{E}} \left\| \frac{\mathbf{Z}_i}{\sqrt{d(v_i)}} - \frac{\mathbf{Z}_j}{\sqrt{d(v_j)}} \right\|_F^2$. As an aftermath, the feature vectors \mathbf{Z} of *heterophilic nodes* (i.e., nodes in different classes) in \mathcal{G} will be made closer (i.e., *over-smoothed*) due to the existence of heterophilic links, and after the clustering operation $\tilde{\mathbf{C}}^\top \mathbf{Z}$, the attribute distances of synthetic heterophilic node pairs in \mathbf{X}' are further reduced. A figurative example to illustrate such a *heterophilic over-smoothing* issue is presented in Fig. 4, wherein the attribute vectors in \mathbf{X}' of synthetic nodes u_1 (merged from $C_1 = \{v_1, \dots, v_5\}$) and u_2 (merged from $C_2 = \{v_6, v_7, v_8\}$) are finally similar to each other, making them hard to distinguish by GNNs. In sum, constructing \mathbf{X}' by Eq. (11) yields over-smoothed attribute vectors and compromises condensation quality.

To validate this issue, we conduct an empirical statistical analysis of \mathbf{X}' on real datasets. Given attribute vectors \mathbf{X} , we define the *inter-class attribute distance* (ICAD) of \mathcal{G} as follows:

$$\phi(\mathbf{X}, \mathbf{Y}) = \frac{1}{2 \sum_{x \neq y} \|Y_{\cdot, x}\|_1 \cdot \|Y_{\cdot, y}\|_1} \sum_{v_i, v_j \in \mathcal{G}, y_i \neq y_j} \left\| \frac{\mathbf{X}_i}{\|\mathbf{X}_i\|_2} - \frac{\mathbf{X}_j}{\|\mathbf{X}_j\|_2} \right\|_2^2,$$

where $\|Y_{\cdot, x}\|_1$ (resp. $\|Y_{\cdot, y}\|_1$) signifies the size of the x -th (resp. y -th) class. $\phi(\mathbf{X}, \mathbf{Y})$ quantifies the averaged distance of attribute vectors \mathbf{X} of heterophilic node pairs. In the same vein, we can define the ICAD of the condensed graph \mathcal{G}' with the synthetic attribute vectors \mathbf{X}' and label matrix \mathbf{Y}' . As reported in Table 1, we can observe a decrease in the ICAD on each dataset, i.e., $\phi(\mathbf{X}', \mathbf{Y}') < \phi(\mathbf{X}, \mathbf{Y})$, which corroborates the foregoing issue of heterophilic over-smoothing in \mathbf{X}' .

Class-Specific Graph Sampling and Representations. To cope with the problematic \mathbf{X}' , we propose to learn a small attribute augmentation Δ to inject class-relevant features into it to build a new attribute matrix for nodes and increase the ICAD, i.e.,

$$\mathbf{X}' + \beta \cdot \Delta, \quad (12)$$

where β stands for the weight of the augmentation. As displayed in Table 1, the ICAD of the synthetic attributes of nodes with this refinement (i.e., Eq. (12)) can be considerably increased, mitigating the heterophilic over-smoothing issue.

Specifically, we sample K graphs $\{A^{(y)}\}_{y=1}^K$ from the original graph \mathcal{G} for the respective classes in \mathcal{Y} , each of which aims to capture the key structural patterns pertinent to its respective class in \mathcal{G} . To achieve this goal, for each class $y \in \mathcal{Y}$, CAAR first reweight each edge (v_i, v_j) in \mathcal{G} by the following weighting scheme:

$$w(v_i, v_j) = P_{i,y} \cdot P_{j,y} \cdot r(v_i, v_j), \quad (13)$$

where $P_{i,y}$ (defined in Eq. (9)) is the predicted probability that the node v_i belongs to the y -th class. As such, $P_{i,y} \cdot P_{j,y}$ in Eq. (13) leads to a low weight $w(v_i, v_j)$ for adjacent nodes (v_i, v_j) that are unlikely to share the same class label, thereby eliminating the impact of heterophilic links.

To account for the importance of each edge (v_i, v_j) in the entire graph topology, we further introduce the well-known *effective resistance* [36] $r(v_i, v_j)$ for (v_i, v_j) in Eq. (13). Instead of computing the exact $r(v_i, v_j)$ over \mathcal{G} , CAAR approximates it on the graph $\tilde{\mathcal{G}}$ constructed from \mathcal{G} with each edge (v_i, v_j) reweighted by $\cos(\mathbf{H}_i, \mathbf{H}_j)$. Note that this reweighting is also to lessen the negative effects of heterophilic links, and the approximation is due to the fact that the exact calculation of $r(v_i, v_j)$ for all edges is prohibitively expensive, particularly for large graphs. More concretely, leveraging the Lemma 4.2 in [27], we can estimate $r(v_i, v_j)$ efficiently by the following equation:

$$r(v_i, v_j) \approx \frac{1}{2} \left(\frac{1}{\tilde{d}(v_i)} + \frac{1}{\tilde{d}(v_j)} \right) \text{ where } \tilde{d}(v_i) = \sum_{v_\ell \in N(v_i)} \cos(\mathbf{H}_i, \mathbf{H}_\ell).$$

After obtaining the weight as in Eq. (13) for each edge in \mathcal{G} , we sample the top- $M \cdot \rho$ ($\rho \in (0, 1)$) ones from \mathcal{E} to construct $A^{(y)}$ instead of retaining all of them. This is to distill the crucial structural features (or homophilic structures) in \mathcal{G} that relate to the class y , while purging noisy and disruptive connections (e.g., heterophilic links).

Based on the K sampled class-specific graphs $\{A^{(y)}\}_{y=1}^K$, we then generate their corresponding K condensed graphs through

$$A^{(y)} = \tilde{C}^\top A^{(y)} \tilde{C}, \quad (14)$$

which leads to K class-specific representation matrices for the n synthetic nodes in \mathcal{G}' :

$$\mathbf{H}'^{(y)} = \sum_{t=0}^{T'} (1 - \alpha) \alpha^t (\mathbf{A}'^{(y)})^t (\mathbf{X}' + \beta \cdot \Delta) \mathbf{W}'. \quad (15)$$

The task then is to learn the features Δ that are commonly missing in the K class-specific representations $\{\mathbf{H}'^{(y)}\}_{y=1}^K$ as augmentation attributes.

Training Losses. To learn Δ and weights \mathbf{W}' , CAAR transforms each $\mathbf{H}'^{(y)}$ into label predictions $\mathbf{P}^{(y)} = \text{Softmax}(\mathbf{H}'^{(y)})$, and adopt the supervision losses \mathcal{L}_{org} , \mathcal{L}_{syn} and consistency loss function \mathcal{L}_{cst} for training:

$$\mathcal{L}_{org} + \gamma \cdot \mathcal{L}_{syn} + \lambda \cdot \mathcal{L}_{cst} \quad (16)$$

where γ and λ are coefficients. \mathcal{L}_{org} is defined as in Eq. (8) and \mathcal{L}_{syn} are implemented using the cross-entropy functions over \mathcal{G}' :

$$\mathcal{L}_{syn} = -\frac{1}{n} \sum_{i=1}^n \sum_{y=1}^K \sum_{k=1}^K Y'_{i,k} \cdot \log(P^{(y)}_{i,k}), \quad (17)$$

where \mathcal{L}_{org} measures the difference between the predicted probability distribution \mathbf{P} and the actual distribution \mathbf{Y} of ground-truth classes on \mathcal{G} , while \mathcal{L}_{syn} calculates that on \mathcal{G}' with the consideration of the K label predictions $\{\mathbf{P}^{(y)}\}_{y=1}^K$.

Additionally, we include the following consistency loss function \mathcal{L}_{cst} [10] as a regularization to encourage an agreement among all class-specific predictions for learning a robust Δ .

$$\mathcal{L}_{cst} = \frac{1}{n \cdot K} \sum_{i=1}^n \sum_{y=1}^K \|\mathbf{P}_i^{(y)} - \bar{\mathbf{P}}\|_2^2 \text{ where } \bar{\mathbf{P}} = \frac{1}{K} \sum_{y=1}^K \mathbf{P}^{(y)}. \quad (18)$$

Algorithm 1: Clustering-based Graph Data Distillation

Input: The original graph \mathcal{G} and label matrix \mathbf{Y}
Output: \mathbf{X}' , \mathbf{A}' , and \mathbf{Y}'

- 1 Generate $\mathbf{Z} = \sum_{t=0}^T (1 - \alpha) \alpha^t \tilde{\mathbf{A}}^t \mathbf{X}$;
- 2 **for** $i = 1$ **to** E_1 **do**
- 3 Predict \mathbf{Y} via $\mathbf{H} = \mathbf{W}\mathbf{Z}$;
- 4 Compute \mathcal{L}_{org} by Eq. (8);
- 5 Generate $\tilde{\mathbf{C}}$ by K -Means on \mathbf{H} with E_2 iterations;
- 6 Get $\mathbf{X}' = \tilde{\mathbf{C}}^\top \mathbf{Z}$, $\mathbf{A}' = \tilde{\mathbf{C}}^\top \tilde{\mathbf{A}} \tilde{\mathbf{C}}$;
- 7 Generate \mathbf{Y}' by taking the argmax of $\tilde{\mathbf{C}}^\top \mathbf{H}$;
- 8 Initialize Δ , update \mathbf{X}' by $\mathbf{X}' = \mathbf{X}' + \beta \cdot \Delta$;
- 9 Generate $\{A^{(y)}\}_{y=1}^K$ according to Eq. (13);
- 10 Get $\{A'^{(y)}\}_{y=1}^K$ and $\{H'^{(y)}\}_{y=1}^K$ by Eq. (14) and (15);
- 11 **for** $i = 1$ **to** E_3 **do**
- 12 Predict \mathbf{Y} via $\mathbf{H}\mathbf{W}'$;
- 13 Predict \mathbf{Y}' via $\mathbf{H}'^{(y)}\mathbf{W}'$;
- 14 Compute \mathcal{L}_{org} , \mathcal{L}_{syn} and \mathcal{L}_{cst} as Eq. (8), (17), (18);
- 15 **return** \mathbf{X}' , \mathbf{A}' , \mathbf{Y}'

5 Pseudo-code and Time Complexity

This section presents the algorithm of ClustGDD as detailed in Algorithm 1. Consider an original graph with M edges, N nodes, d -dimensional attributes, and K classes. Let n denote the clustering number (i.e., synthetic node count), E_1, E_2, E_3 denote epochs for pretraining, clustering, and refinement, T, T' denote propagation iterations in pretraining and refinement. The computational complexity of our framework includes: propagation ($O(MdT)$), mini-batch pretraining ($O(E_1NdK)$), K -means clustering ($O(E_2Nnd)^2$), generating \mathbf{X}' , \mathbf{A}' , and \mathbf{Y}' ($O(Nd + M + NK)$), multi-view graphs generation ($O(K^2M + KM \log M + KM)$), propagation on condensed graphs ($O(Kn^2dT')$), and refinement training ($O(E_3NKd + E_3K^2nd)$). Assuming $E_1, E_2, E_3 = O(E)$, $T, T' = O(1)$, $K = O(1)$, the time complexity simplifies to $O(ENnd + n^2d + Md + M \log M)$. In fact, our

²For large-scale datasets, the mini-batch K -means algorithm is employed with a computational complexity of $O(E_2bnd)$, where b is the batch size.

Table 2: Statistics of Datasets.

Dataset	N	M	d	K
<i>Cora</i>	2,708	5,429	1,433	7
<i>Citeseer</i>	3,327	4,732	3,703	6
<i>Flickr</i>	89,250	899,756	128	7
<i>arXiv</i>	169,343	1,166,243	128	40
<i>Reddit</i>	232,965	57,307,946	602	41

method has a much lower time complexity compared to the baselines, which is analyzed in Appendix B. This is the reason why our method has a very low time cost empirically as shown in the following experiments.

6 Experiments

In this section, we experimentally evaluate our proposed GDD method ClustGDD against nine competitors over five real graphs in terms of node classification performance and efficiency. For reproducibility, the source code and datasets are available at <https://github.com/HKBU-LAGAS/ClustGDD>.

6.1 Experiment Settings

Datasets. Table 2 lists the statistics of the five real graph datasets used in our experiments. *Cora* [40], *Citeseer* [40], and *arXiv* [21] are the classic datasets for transductive node classification, while *Flickr* [57] and *Reddit* [18] are for inductive tasks.

Baselines and Settings. We evaluate our ClustGDD against three classic coreset methods: Random [47], Herding [47] and K-Center [41], and six GDD baselines as categorized below:

- *Gradient Matching*: Gcond [25], SGDD [54], and GCSR [34];
- *Trajectory Matching*: SFGC [59];
- *Eigenbasis Matching*: GDEM [32];
- *Performance Matching*: GC-SNTK [44]

For a fair comparison, we follow the evaluation protocol and settings (e.g., condensation ratios, GNNs, etc.) commonly adopted in previous works [25, 32] for all evaluated methods. We reproduce the performance of Gcond, SFGC, GCSR, and GDEM using the source codes, hyperparameter settings, and synthetic datasets provided by the respective authors. As for the rest of the baselines, we directly use the results reported in [34, 45]. For the interest of space, we defer the details of datasets, implementation, and hyper-parameter settings to Appendix C, and additional experiments on hyper-parameter analysis and visualization to Appendix D.

6.2 Condensation Effectiveness Evaluation

We conduct comprehensive comparison of node classification performance across various coreset and distillation methods. We train GCN on the synthetic graphs and record the test accuracy for evaluation. The ratio is defined as n/N for transductive datasets, and it is defined as $n/N_{\mathcal{T}}$ for the inductive ones, where $N_{\mathcal{T}}$ is the number of training nodes.

We can summarize several key points from the results shown in Table 3. Firstly, Our ClustGDD and ClustGDD-X obtain overall highest/second-highest accuracy on most datasets, and sometimes

higher than the results of the whole datasets. For instance, on *Citeseer*, the average accuracy of ClustGDD on three ratios is 74.2%, which is 2.4% higher than original result. We suggest that the success of ClustGDD can be primarily attributed to two key factors: during the clustering phase, ClustGDD effectively integrates information from both the original attributes and the graph topology through GLS. Through pretraining and clustering, the FID between the condensed attributes and the original attributes is minimized. On the other hand, during the refinement phase, the condensed attributes are further improved by co-training on original and condensed graphs, reducing the Heterophilic Over-smoothing Issue. Secondly, the results of ClustGDD are slightly better than ClustGDD-X, indicating that the synthetic attributes capture most of the original graph’s key information, with the synthetic topology offering supplementary advantages. We also find distillation methods consistently outperform traditional methods, demonstrating the overall effectiveness and robustness of distillation methods.

We present the average time costs of coreset and GDD methods across five datasets with condensation ratios of 2.6%, 1.8%, 0.05%, 0.10%, and 0.10%, respectively. Experimental findings reveal a notable trade-off: while traditional graph distillation methods achieve high node classification accuracy, their computational overhead remains prohibitive (ranging from 10^3 to 10^4 seconds). Conversely, coreset methods demonstrate remarkable efficiency (approximately 92 seconds) at the cost of diminished accuracy. Our proposed ClustGDD method effectively bridges this gap, achieving state-of-the-art accuracy in merely 56.8 seconds. Detailed per-dataset performance metrics are available in Appendix D.

6.3 Cross-architecture Generalization

To verify the generalization of our distilled graph, we use different GNN architectures to train on synthetic graphs and test their performance on the original graph, and the results are shown in Table 4. ClustGDD achieves the overall highest average, and the lowest std, showing its stability and effectiveness when datasets and GNNs architecture vary. For example, on the *arXiv* dataset, the average accuracy of our method is 2.8% higher than that of the second-place, GCSR, and the std is reduced by 1.7%. This validates that ClustGDD has the superior generalization ability across GDDs. This may be because the closed-form solution of GLS in the clustering and refinement is more stable than other specific GNNs.

6.4 Ablation Study

Varying Clustering Methods. We use different GNNs architectures to replace the closed-form solution of GLS as the backbone in the pretraining and refinement stages. In general, SGC and APPNP perform well on the *Cora* and *Citeseer*. ChebyNet shows good performance on the *arXiv* and *Reddit* datasets. MLP has the highest accuracy on the *Flickr* dataset. Our backbone consistently outperforms the others across all datasets, this may be attributed to several key factors. Firstly, it excels at capturing the global structure of graphs, allowing it to model long-range dependencies and overall connectivity patterns effectively, which is crucial in datasets where important features are spread across the entire graph. Secondly, it assigns weighted influence to nodes based on their importance, enabling the model to focus more on key nodes that drive the graph

Table 3: Node classification performance (mean accuracy (%), \pm standard deviation) and average dataset synthesis time (second) of ClustGDD and baselines. (best is highlighted in blue and runner-up in light-blue). The results of methods with * are taken from prior works.

Dataset	Ratio	Coreset Methods				GDD Methods							Whole Dataset
		Random	Herding	K-Center	Gcond	SFGC	SGDD*	GCSR	GC-SNTK*	GDEM	ClustGDD-X	ClustGDD	
Cora	1.30%	62.3 \pm 1.1	68.0 \pm 0.6	62.5 \pm 0.7	80.6 \pm 0.8	79.9 \pm 0.5	79.1 \pm 1.3	79.7 \pm 1.4	81.7 \pm 0.7	78.7 \pm 3.1	81.0 \pm 0.4	80.8 \pm 0.3	81.1 \pm 0.4
	2.60%	73.1 \pm 0.9	73.4 \pm 0.4	73.3 \pm 0.5	81.1 \pm 0.5	80.7 \pm 0.3	79.0 \pm 1.9	81.1 \pm 0.4	81.5 \pm 0.7	77.7 \pm 1.0	81.6 \pm 0.6	81.7 \pm 0.5	
	5.20%	76.5 \pm 0.4	76.6 \pm 0.4	77.0 \pm 0.4	80.7 \pm 0.6	80.3 \pm 0.4	80.2 \pm 0.8	80.8 \pm 0.7	81.3 \pm 0.2	80.3 \pm 1.0	82.4 \pm 0.5	83.0 \pm 0.3	
Citeseer	0.90%	49.7 \pm 0.7	55.8 \pm 0.6	48.8 \pm 1.1	72.3 \pm 0.5	70.5 \pm 0.4	71.5 \pm 0.9	71.1 \pm 0.9	64.8 \pm 0.7	72.9 \pm 0.7	73.5 \pm 0.2	73.5 \pm 0.2	71.8 \pm 0.3
	1.80%	57.7 \pm 0.7	68.2 \pm 0.4	65.2 \pm 0.6	72.5 \pm 0.6	71.8 \pm 0.1	71.2 \pm 0.7	71.4 \pm 0.5	65.9 \pm 0.2	74.4 \pm 0.3	74.4 \pm 0.2	74.4 \pm 0.2	
	3.60%	69.0 \pm 0.5	69.0 \pm 0.8	69.5 \pm 0.5	70.9 \pm 0.5	71.1 \pm 0.5	70.9 \pm 1.2	73.0 \pm 0.6	66.3 \pm 0.5	74.1 \pm 1.1	74.5 \pm 0.5	74.6 \pm 0.3	
arXiv	0.05%	43.8 \pm 1.5	51.8 \pm 1.2	48.0 \pm 1.4	56.4 \pm 2.5	63.3 \pm 0.7	59.6 \pm 0.5	60.7 \pm 0.7	64.2 \pm 0.2	61.8 \pm 1.8	63.7 \pm 0.4	63.7 \pm 0.1	71.1 \pm 0.2
	0.25%	57.0 \pm 0.7	60.5 \pm 0.7	56.4 \pm 0.8	60.7 \pm 2.2	67.3 \pm 0.7	61.7 \pm 0.3	64.4 \pm 0.3	65.1 \pm 0.8	61.8 \pm 0.4	67.4 \pm 0.3	67.5 \pm 0.1	
	0.50%	58.8 \pm 0.8	60.5 \pm 0.4	60.1 \pm 0.5	60.9 \pm 2.0	67.9 \pm 0.2	58.7 \pm 0.6	66.4 \pm 0.3	65.4 \pm 0.5	63.3 \pm 0.5	67.6 \pm 0.1	67.7 \pm 0.2	
Flickr	0.10%	42.0 \pm 0.3	40.5 \pm 0.7	41.3 \pm 0.7	46.3 \pm 0.6	46.7 \pm 0.2	46.1 \pm 0.3	46.6 \pm 0.2	46.7 \pm 0.1	45.7 \pm 0.6	46.8 \pm 0.1	46.9 \pm 0.1	46.9 \pm 0.1
	0.50%	42.9 \pm 0.5	42.7 \pm 0.4	43.6 \pm 0.3	46.9 \pm 0.1	47.2 \pm 0.1	45.9 \pm 0.4	46.7 \pm 0.1	46.8 \pm 0.1	46.1 \pm 0.6	46.8 \pm 0.1	46.9 \pm 0.1	
	1.00%	42.8 \pm 0.6	44.9 \pm 0.2	43.9 \pm 0.5	47.1 \pm 0.3	46.9 \pm 0.2	46.4 \pm 0.2	46.9 \pm 0.3	46.5 \pm 0.2	46.4 \pm 0.4	46.9 \pm 0.2	47.1 \pm 0.1	
Reddit	0.05%	44.8 \pm 1.4	52.2 \pm 1.3	48.5 \pm 0.7	87.2 \pm 0.9	78.8 \pm 1.3	84.2 \pm 0.7	90.5 \pm 0.3	74.3 \pm 0.5	91.4 \pm 0.4	89.8 \pm 0.1	89.8 \pm 0.1	94.1 \pm 0.0
	0.10%	60.2 \pm 1.3	61.4 \pm 1.0	49.0 \pm 1.2	89.1 \pm 0.8	80.7 \pm 1.9	90.7 \pm 0.1	91.2 \pm 0.4	74.8 \pm 0.7	91.5 \pm 0.4	91.5 \pm 0.1	91.5 \pm 0.1	
	0.50%	79.3 \pm 1.0	82.1 \pm 0.2	70.3 \pm 0.7	90.1 \pm 0.7	87.1 \pm 0.3	—	84.6 \pm 1.1	85.2 \pm 1.2	91.4 \pm 0.7	91.6 \pm 0.0	91.7 \pm 0.0	
Avg. Time		92.4	92.6	92.0	8,150.4	104,999.0	46,424.8	4,350.4	3,045.4	1,316.4	56.7	56.8	

Table 4: Generalization of GDD methods across GNNs.

Dataset	Method	GNN Architectures					Avg.	Std.
		GCN	SGC	APNP	ChebyNet	BernNet		
Cora	Gcond	81.1	81.0	80.2	60.8	81.0	76.8	8.0
	SFGC	80.7	80.7	80.2	81.8	80.2	80.7	0.6
	GCSR	81.1	81.4	81.4	82.3	82.0	81.6	0.4
	GDEM	77.7	77.8	78.0	77.3	78.2	77.8	0.3
	ClustGDD	81.7	82.1	81.7	82.3	82.3	82.0	0.3
Citeseer	Gcond	72.5	71.7	71.6	33.5	70.3	63.9	15.2
	SFGC	71.8	71.8	71.3	70.3	66.6	70.4	2.0
	GCSR	71.4	71.6	71.6	66.0	63.9	68.9	3.3
	GDEM	74.4	74.6	74.7	73.1	72.1	73.8	1.0
	ClustGDD	74.4	74.3	74.6	73.3	73.1	73.9	0.6
arXiv	Gcond	56.4	46.4	58.0	46.4	59.1	53.3	5.7
	SFGC	63.3	60.7	55.7	61.6	60.2	60.3	2.5
	GCSR	60.7	55.7	58.7	61.4	61.3	59.6	2.2
	GDEM	61.8	60.4	59.2	60.5	56.8	59.7	1.7
	ClustGDD	63.7	61.9	62.4	64.0	63.3	63.1	0.8
Flickr	Gcond	46.3	46.3	44.9	41.8	38.1	43.5	3.2
	SFGC	46.7	46.5	46.7	46.4	45.4	46.3	0.5
	GCSR	46.6	46.5	46.6	46.2	45.6	46.3	0.4
	GDEM	45.7	44.5	44.4	44.2	40.1	43.8	1.9
	ClustGDD	46.9	46.9	46.7	46.5	46.4	46.7	0.2
Reddit	Gcond	89.1	89.9	87.5	21.1	87.3	75.0	27.0
	SFGC	80.7	62.4	62.6	78.5	75.0	71.8	7.8
	GCSR	91.2	89.3	87.2	70.4	85.5	84.7	7.4
	GDEM	91.5	91.4	91.0	85.8	82.2	88.4	3.8
	ClustGDD	91.5	90.7	88.7	87.5	83.9	88.5	2.7

dynamics and aggregate their features more meaningfully. These combined strengths enable the personalized PageRank backbone to consistently deliver superior performance across diverse datasets.

Attribute Refinement. We then explore the impact of modules in CAAR. Firstly, we remove the refinement (w/o CAAR), using synthetic attributes and topology from the clustering stage to train

Table 5: Ablation study results.

Modules	Cora	Citeseer	arXiv	Flickr	Reddit
w/ MLP	77.8 \pm 0.7	72.3 \pm 0.3	58.7 \pm 0.4	45.5 \pm 0.4	81.6 \pm 0.3
w/ GCN	78.9 \pm 0.5	70.9 \pm 0.7	60.9 \pm 0.3	43.6 \pm 1.1	87.7 \pm 0.4
w/ SGC	81.7 \pm 0.5	72.3 \pm 0.3	57.5 \pm 0.7	45.1 \pm 0.7	77.7 \pm 0.3
w/ APNP	80.6 \pm 0.2	72.2 \pm 0.3	59.4 \pm 0.6	41.4 \pm 1.2	86.3 \pm 0.1
w/ BernNet	79.2 \pm 0.4	72.0 \pm 0.1	58.7 \pm 0.5	45.0 \pm 0.2	84.6 \pm 0.4
w/ ChebyNet	79.5 \pm 0.4	72.1 \pm 0.6	61.4 \pm 0.2	45.8 \pm 0.1	87.2 \pm 0.4
w/o CAAR	81.3 \pm 0.4	74.0 \pm 0.3	61.9 \pm 0.4	46.3 \pm 0.2	87.6 \pm 0.2
w/o sampling	81.5 \pm 0.2	74.1 \pm 0.2	62.6 \pm 0.3	46.8 \pm 0.1	90.4 \pm 0.1
w/o \mathcal{L}_{cst}	81.6 \pm 0.5	74.3 \pm 0.2	63.5 \pm 0.3	46.7 \pm 0.1	91.4 \pm 0.1
ClustGDD	81.7 \pm 0.5	74.4 \pm 0.2	63.7 \pm 0.1	46.9 \pm 0.1	91.5 \pm 0.1

GNNs, it leads to a decline in GNN performance across all datasets, especially on datasets with a higher compression ratio and class imbalance, such as *Reddit* and *arXiv*. Secondly, we replace the multiple representations $\{H^{(y)}\}_{y=1}^K$ created via class-specific sampled graphs in CAAR by a single H' (w/o sampling). Due to the lack of information from different views, the performance of GNN declines across all datasets, especially on large graphs such as *Reddit* and *arXiv*. Then, we remove the consistency loss (w/o \mathcal{L}_{cst}). It indeed affects the quality of the distilled graph. It's because the consistency of predictions enhances the robustness of the refinement.

6.5 Hyper-parameter Analysis

Next, we conduct hyper-parameter analysis in our method on *arXiv* and *Reddit*, evaluating the impact of various hyperparameters on the performance of our machine learning model in Fig. 5. First, we explore the propagation number T in of the pretraining stage,

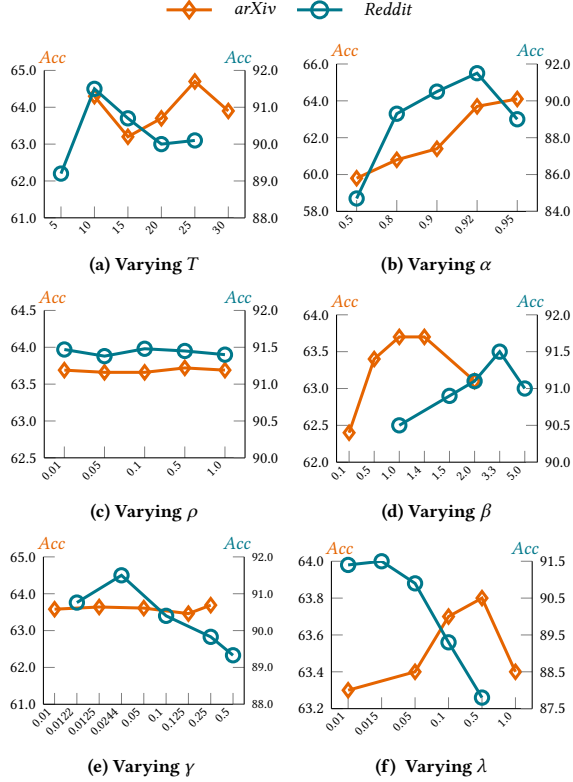


Figure 5: Hyper-parameter Analysis.

which is critical for controlling the degree of information integration between nodes at different distances in the graph. The model’s performance initially increases with T and then decreases on both *arXiv* and *Reddit*. This means that aggregating information from nearby neighbors is beneficial, while excessive message passing may lead to over-smoothing, resulting in a decline in performance. Then we tune another hyper-parameter α , α represents the weight between exploring neighbors and back to a starting node. A larger α means the model is more likely to explore, leading to results that are influenced by the overall graph structure, which is important for the task on relatively larger graphs. We find that when generating multi-view representations, a certain degree of sparsity ρ can help the model achieve optimal performance, and our method is relatively robust to varying levels of sparsity. We find that the strength of the refinement on attributes, represented by β , significantly affect the quality of the distilled graph attributes, thereby influencing the model’s performance. In refinement, we find that adjusting the coefficient γ for the supervision loss has a greater impact than adjusting the coefficient λ for the consistency loss. This suggests that the supervision loss on multi-view graphs may be more important.

7 Related Work

Graph Data Distillation (GDD). Unlike conventional *graph reduction* approaches, such as *coreset selection*, *graph sparsification*, and *coarsening*, GDD achieves encouraging performance due to the mechanism of leveraging the gradients/representation of GNNs in

downstream tasks for graph dataset synthesis, which can be roughly categorized into several types. Among gradient matching, GCond [25], DosCond [24] align gradient signals between original and condensed graphs to ensure model performance transfer. SGDD [54], and GCSR [34] are another two structure-aware gradient-based methods, preserving essential topology information. However, gradient matching needs nested optimization, making the balance between high condensation costs and low condensation quality difficult. Training trajectory matching approaches like SFGC [59] preserve GNN learning consistency through long-term trajectory alignment but incur high computational costs in expert model training. Distribution matching methods (GCDM [31], SimGC [50]) iteratively align representation distributions between synthetic and original graphs, resulting in suboptimal efficiency. Eigen matching methods such as GDEM [32] maintain graph spectral properties through eigen-decomposition alignment, yet struggle with scalability for large graphs. Performance matching (GC-SNTK [44], KiDD [53]) provide closed-form solutions via kernel regression but suffer from prohibitive memory demands for kernel matrix storage. Gradient-free methods like CGC [14] employ clustering-based feature matching but sacrifice task-specific adaptability by avoiding gradient optimization. While existing works explore diverse graph condensation paradigms, they exhibit limitations in computational efficiency (trajectory/eigen decomposition costs), memory consumption (kernel matrices), or optimization flexibility (lack of gradient guidance). These bottlenecks motivate us to design an efficient, structure-aware, and optimization-friendly GDD method.

Data Distillation. Dataset distillation [28, 38, 39] is a technique that compresses the knowledge of a large dataset into a smaller, synthetic dataset, enabling models to be trained with less data while maintaining comparable performance to models trained on the original dataset. It is not only applied to graph data, but also widely used in other fields e.g., such as visual datasets [55, 56] and text datasets [30, 43]. For example, DaLLME [43] compresses two text datasets *IMDB* and *AG-News* to 0.1% via language model embedding, with text classification loss decreases less than 10%. Designing unified data distillation methods for multi-modal data will be a promising direction.

8 Conclusion

This paper proposes a simple yet effective approach ClustGDD for GDD. ClustGDD achieves superior performance in condensation effectiveness and efficiency over previous GDD solutions on real datasets through two major contributions: a simple clustering method minimizing the WCSS and a lightweight module augmenting synthetic attributes with class-relevant features. As for future work, we intend to extend our solutions to handle graphs that are heterogeneous or from multiple modalities.

Acknowledgments

This work is supported by the National Natural Science Foundation of China (No. 62302414), the Hong Kong RGC ECS grant (No. 22202623), and the Huawei Gift Fund.

References

- [1] Huzihiro Araki. 1990. On an inequality of Lieb and Thirring. *Letters in Mathematical Physics* 19, 2 (1990), 167–170.
- [2] Fedor Borisjuk, Shihai He, Yunbo Ouyang, Morteza Ramezani, Peng Du, Xiaochen Hou, Chengming Jiang, Nitin Pasumarthy, Priya Bannur, Birjodh Tiwana, et al. 2024. Lignn: Graph neural networks at linkedin. In *Proceedings of the 30th ACM SIGKDD Conference on Knowledge Discovery and Data Mining*. 4793–4803.
- [3] Yingmei Chen, Zhongyu Wei, and Xuanjing Huang. 2018. Incorporating corporation relationship via graph convolutional neural networks for stock price prediction. In *CIKM*. 1655–1658.
- [4] Michaël Defferrard, Xavier Bresson, and Pierre Vandergheynst. 2016. Convolutional neural networks on graphs with fast localized spectral filtering. *Advances in neural information processing systems* 29 (2016).
- [5] Austin Darrow-Pinion, Jennifer She, David Wong, Oliver Lange, Todd Hester, Luis Perez, Marc Nunkesser, Seongjae Lee, Xueying Guo, Brett Wiltshire, et al. 2021. Eta prediction with graph neural networks in google maps. In *CIKM*. 3767–3776.
- [6] Mucong Ding, Xiaoyu Liu, Tahseen Rabbani, and Furong Huang. 2022. Faster hyperparameter search on graphs via calibrated dataset condensation. In *NeurIPS 2022 Workshop: New Frontiers in Graph Learning*.
- [7] Xiaowen Dong, Dorina Thanou, Pascal Frossard, and Pierre Vandergheynst. 2016. Learning Laplacian matrix in smooth graph signal representations. *IEEE Transactions on Signal Processing* 64, 23 (2016), 6160–6173.
- [8] DC Dowson and BV66017 Landau. 1982. The Fréchet distance between multivariate normal distributions. *Journal of multivariate analysis* 12, 3 (1982), 450–455.
- [9] Junfeng Fang, Xinglin Li, Yongduo Sui, Yuan Gao, Guibin Zhang, Kun Wang, Xiang Wang, and Xiangnan He. 2024. Exgc: Bridging efficiency and explainability in graph condensation. In *Proceedings of the ACM on Web Conference 2024*. 721–732.
- [10] Wenzheng Feng, Jie Zhang, Yuxiao Dong, Yu Han, Huanbo Luan, Qian Xu, Qiang Yang, Evgeny Kharlamov, and Jie Tang. 2020. Graph random neural networks for semi-supervised learning on graphs. *Advances in neural information processing systems* 33 (2020), 22092–22103.
- [11] Alex Fout, Jonathon Byrd, Basir Shariat, and Asa Ben-Hur. 2017. Protein interface prediction using graph convolutional networks. In *Proceedings of the 31st International Conference on Neural Information Processing Systems*. 6533–6542.
- [12] Chen Gao, Yu Zheng, Nian Li, Yinfeng Li, Yingrong Qin, Jinghua Piao, Yuhuan Quan, Jianxin Chang, Depeng Jin, Xiangnan He, et al. 2023. A survey of graph neural networks for recommender systems: Challenges, methods, and directions. *ACM Transactions on Recommender Systems* 1, 1 (2023), 1–51.
- [13] Xinyi Gao, Tong Chen, Yilong Zang, Wentao Zhang, Quoc Viet Hung Nguyen, Kai Zheng, and Hongzhi Yin. 2024. Graph condensation for inductive node representation learning. In *2024 IEEE 40th International Conference on Data Engineering (ICDE)*. IEEE, 3056–3069.
- [14] Xinyi Gao, Tong Chen, Wentao Zhang, Junliang Yu, Guanhua Ye, Quoc Viet Hung Nguyen, and Hongzhi Yin. 2024. Rethinking and Accelerating Graph Condensation: A Training-Free Approach with Class Partition. *arXiv preprint arXiv:2405.13707* (2024).
- [15] Xinyi Gao, Junliang Yu, Tong Chen, Guanhua Ye, Wentao Zhang, and Hongzhi Yin. 2025. Graph condensation: A survey. *IEEE Transactions on Knowledge and Data Engineering* (2025).
- [16] Johannes Gasteiger, Aleksandar Bojchevski, and Stephan Günnemann. 2018. Predict then Propagate: Graph Neural Networks meet Personalized PageRank. In *International Conference on Learning Representations*.
- [17] Justin Gilmer, Samuel S Schoenholz, Patrick F Riley, Oriol Vinyals, and George E Dahl. 2017. Neural message passing for quantum chemistry. In *International conference on machine learning*. PMLR, 1263–1272.
- [18] Will Hamilton, Zhitaoying, and Jure Leskovec. 2017. Inductive representation learning on large graphs. *Advances in neural information processing systems* 30 (2017).
- [19] Mohammad Hashemi, Shengbo Gong, Juntong Ni, Wenqi Fan, B Aditya Prakash, and Wei Jin. 2024. A comprehensive survey on graph reduction: Sparsification, coarsening, and condensation. *arXiv preprint arXiv:2402.03358* (2024).
- [20] Martin Heusel, Hubert Ramsauer, Thomas Unterthiner, Bernhard Nessler, and Sepp Hochreiter. 2017. Gans trained by a two time-scale update rule converge to a local nash equilibrium. *Advances in neural information processing systems* 30 (2017).
- [21] Weihua Hu, Matthias Fey, Marinka Zitnik, Yuxiao Dong, Hongyu Ren, Bowen Liu, Michele Catasta, and Jure Leskovec. 2020. Open graph benchmark: Datasets for machine learning on graphs. *Advances in neural information processing systems* 33 (2020), 22118–22133.
- [22] Dejun Jiang, Zhenxing Wu, Chang-Yu Hsieh, Guangyong Chen, Ben Liao, Zhe Wang, Chao Shen, Dongsheng Cao, Jian Wu, and Tingjun Hou. 2021. Could graph neural networks learn better molecular representation for drug discovery? A comparison study of descriptor-based and graph-based models. *Journal of cheminformatics* 13 (2021), 1–23.
- [23] Weiwei Jiang and Jiayun Luo. 2022. Graph neural network for traffic forecasting: A survey. *ESA* 207 (2022), 117921.
- [24] Wei Jin, Xianfeng Tang, Haoming Jiang, Zheng Li, Danqing Zhang, Jiliang Tang, and Bing Yin. 2022. Condensing graphs via one-step gradient matching. In *Proceedings of the 28th ACM SIGKDD Conference on Knowledge Discovery and Data Mining*. 720–730.
- [25] Wei Jin, Lingxiao Zhao, Shichang Zhang, Yozen Liu, Jiliang Tang, and Neil Shah. 2021. Graph condensation for graph neural networks. *arXiv preprint arXiv:2110.07580* (2021).
- [26] Thomas N Kipf and Max Welling. 2016. Semi-supervised classification with graph convolutional networks. *arXiv preprint arXiv:1609.02907* (2016).
- [27] Yurui Lai, Xiaoyang Lin, Renchi Yang, and Hongtao Wang. 2024. Efficient topology-aware data augmentation for high-degree graph neural networks. In *Proceedings of the 30th ACM SIGKDD Conference on Knowledge Discovery and Data Mining*. 1463–1473.
- [28] Shiye Lei and Dacheng Tao. 2023. A comprehensive survey of dataset distillation. *IEEE Transactions on Pattern Analysis and Machine Intelligence* (2023).
- [29] Fan Li, Xiaoyang Wang, Dawei Cheng, Wenjie Zhang, Ying Zhang, and Xuemin Lin. 2024. TCGU: Data-centric Graph Unlearning based on Transferable Condensation. *arXiv preprint arXiv:2410.06480* (2024).
- [30] Yongqi Li and Wenjie Li. 2021. Data distillation for text classification. *arXiv preprint arXiv:2104.08448* (2021).
- [31] Mengyang Liu, Shanchuan Li, Xinshi Chen, and Le Song. 2022. Graph condensation via receptive field distribution matching. *arXiv preprint arXiv:2206.13697* (2022).
- [32] Yang Liu, Deyu Bo, and Chuan Shi. 2024. Graph Distillation with Eigenbasis Matching. In *Forty-first International Conference on Machine Learning*.
- [33] Yilun Liu, Ruihong Qiu, and Zi Huang. 2023. Cat: Balanced continual graph learning with graph condensation. In *2023 IEEE International Conference on Data Mining (ICDM)*. IEEE, 1157–1162.
- [34] Zhanyu Liu, Chaolv Zeng, and Guanjie Zheng. 2024. Graph data condensation via self-expressive graph structure reconstruction. In *Proceedings of the 30th ACM SIGKDD Conference on Knowledge Discovery and Data Mining*. 1992–2002.
- [35] Stuart Lloyd. 1982. Least squares quantization in PCM. *IEEE transactions on information theory* 28, 2 (1982), 129–137.
- [36] László Lovász. 1993. Random walks on graphs. *Combinatorics, Paul erdos is eighty* 2, 1–46 (1993), 4.
- [37] Yao Ma, Xiaorui Liu, Tong Zhao, Yozen Liu, Jiliang Tang, and Neil Shah. 2021. A unified view on graph neural networks as graph signal denoising. In *Proceedings of the 30th ACM International Conference on Information & Knowledge Management*. 1202–1211.
- [38] Ilija Radosavovic, Piotr Dollár, Ross Girshick, Georgia Gkioxari, and Kaiming He. 2018. Data distillation: Towards omni-supervised learning. In *Proceedings of the IEEE conference on computer vision and pattern recognition*. 4119–4128.
- [39] Naveen Sachdeva and Julian McAuley. 2023. Data distillation: A survey. *arXiv preprint arXiv:2301.04272* (2023).
- [40] Prithviraj Sen, Galileo Namata, Mustafa Bilgic, Lise Getoor, Brian Galligher, and Tina Eliassi-Rad. 2008. Collective classification in network data. *AI magazine* 29, 3 (2008), 93–93.
- [41] Ozan Sener and Silvio Savarese. 2017. Active learning for convolutional neural networks: A core-set approach. *arXiv preprint arXiv:1708.00489* (2017).
- [42] Jonathan M Stokes, Kevin Yang, Kyle Swanson, Wengong Jin, Andres Cubillos-Ruiz, Nina M Donghia, Craig R MacNair, Shawn French, Lindsey A Carfrae, Zohar Bloom-Ackermann, et al. 2020. A deep learning approach to antibiotic discovery. *Cell* 180, 4 (2020), 688–702.
- [43] Yefan Tao, Luyang Kong, Andrey Kan, and Laurent Collobert. 2024. Textual Dataset Distillation via Language Model Embedding. In *Findings of the Association for Computational Linguistics: EMNLP 2024*. 12557–12569.
- [44] Lin Wang, Wenqi Fan, Jiatong Li, Yao Ma, and Qing Li. 2024. Fast graph condensation with structure-based neural tangent kernel. In *Proceedings of the ACM on Web Conference 2024*. 4439–4448.
- [45] Lin Wang and Qing Li. 2025. Efficient Graph Condensation via Gaussian Process. *arXiv preprint arXiv:2501.02565* (2025).
- [46] Yuyang Wang, Jianren Wang, Zhonglin Cao, and Amir Barati Farimani. 2022. Molecular contrastive learning of representations via graph neural networks. *Nature Machine Intelligence* 4, 3 (2022), 279–287.
- [47] Max Welling. 2009. Herding dynamical weights to learn. In *Proceedings of the 26th annual international conference on machine learning*. 1121–1128.
- [48] Lirong Wu, Haitao Lin, Zhangyang Gao, Guojiang Zhao, and Stan Z. Li. 2024. A Teacher-Free Graph Knowledge Distillation Framework With Dual Self-Distillation. *IEEE Transactions on Knowledge and Data Engineering* 36, 9 (2024), 4375–4385. <https://doi.org/10.1109/TKDE.2024.3374773>
- [49] Shiwen Wu, Fei Sun, Wentao Zhang, Xu Xie, and Bin Cui. 2022. Graph neural networks in recommender systems: a survey. *Comput. Surveys* 55, 5 (2022), 1–37.
- [50] Zhenbang Xiao, Yu Wang, Shunyu Liu, Huiqiong Wang, Mingli Song, and Tongya Zheng. 2024. Simple graph condensation. In *Joint European Conference on Machine Learning and Knowledge Discovery in Databases*. Springer, 53–71.
- [51] Hongjia Xu, Liangliang Zhang, Yao Ma, Sheng Zhou, Zhuonan Zheng, and Bu Jiajun. 2024. A survey on graph condensation. *arXiv preprint arXiv:2402.02000* (2024).

- [52] Keyulu Xu, Chengtao Li, Yonglong Tian, Tomohiro Sonobe, Ken-ichi Kawarabayashi, and Stefanie Jegelka. 2018. Representation learning on graphs with jumping knowledge networks. In *International conference on machine learning*. PMLR, 5453–5462.
- [53] Zhe Xu, Yuzhong Chen, Menghai Pan, Huiyuan Chen, Mahashweta Das, Hao Yang, and Hanghang Tong. 2023. Kernel ridge regression-based graph dataset distillation. In *Proceedings of the 29th ACM SIGKDD Conference on Knowledge Discovery and Data Mining*. 2850–2861.
- [54] Beining Yang, Kai Wang, Qingyun Sun, Cheng Ji, Xingcheng Fu, Hao Tang, Yang You, and Jianxin Li. 2023. Does graph distillation see like vision dataset counterpart? *Advances in Neural Information Processing Systems* 36 (2023), 53201–53226.
- [55] Zeyuan Yin and Zhiqiang Shen. 2024. Dataset distillation via curriculum data synthesis in large data era. *Transactions on Machine Learning Research* (2024).
- [56] Zeyuan Yin, Eric Xing, and Zhiqiang Shen. 2024. Squeeze, recover and relabel: Dataset condensation at imagenet scale from a new perspective. *Advances in Neural Information Processing Systems* 36 (2024).
- [57] Hanqing Zeng, Hongkuan Zhou, Ajitesh Srivastava, Rajgopal Kannan, and Viktor Prasanna. 2019. Graphsaint: Graph sampling based inductive learning method. *arXiv preprint arXiv:1907.04931* (2019).
- [58] Ge Zhang, Zhao Li, Jiaming Huang, Jia Wu, Chuan Zhou, Jian Yang, and Jianliang Gao. 2022. efraudcom: An e-commerce fraud detection system via competitive graph neural networks. *TOIS* 40, 3 (2022), 1–29.
- [59] Xin Zheng, Miao Zhang, Chunyang Chen, Quoc Viet Hung Nguyen, Xingquan Zhu, and Shirui Pan. 2024. Structure-free graph condensation: From large-scale graphs to condensed graph-free data. *Advances in Neural Information Processing Systems* 36 (2024).
- [60] Ziang Zhou, Jieming Shi, Renchi Yang, Yuanhang Zou, and Qing Li. 2023. SlotGAT: slot-based message passing for heterogeneous graphs. In *International Conference on Machine Learning*. PMLR, 42644–42657.
- [61] Jiong Zhu, Yujun Yan, Lingxiao Zhao, Mark Heimann, Leman Akoglu, and Danai Koutra. 2020. Beyond homophily in graph neural networks: Current limitations and effective designs. *Advances in neural information processing systems* 33 (2020), 7793–7804.
- [62] Meiqi Zhu, Xiao Wang, Chuan Shi, Houye Ji, and Peng Cui. 2021. Interpreting and Unifying Graph Neural Networks with An Optimization Framework. *Proceedings of the Web Conference 2021* (2021).

A A Detailed Discussion of Existing GDD Works

We here provide a concise formalization of some representative GDD methods.

Gradient matching. e.g. GCond [25] optimizes the synthetic graphs by minimizing the difference between the gradients of GNNs on original and synthetic graphs.

$$\min_{\mathcal{G}'} \mathbb{E}_{\Theta \sim \mathcal{P}_\Theta} \left[\sum_{l=1}^L D(\nabla_{\Theta} \mathcal{L}(\text{GNN}_{\Theta}(A', X'), Y'), \nabla_{\Theta} \mathcal{L}(\text{GNN}_{\Theta}(A, X), Y)) \right]$$

$$s.t. \quad \Theta_{\mathcal{G}'} = \arg \min_{\Theta} \mathcal{L}(\text{GNN}_{\Theta}(A', X'), Y')$$

where L is the number of matching steps. In fact, GCond involves a nested optimization. It optimizes the synthetic dataset within the inner loop and trains the GNNs on the original graph in the outer loop, which makes the training process very time-consuming.

Distribution matching. GCDM [31] minimizes the distance between distribution of GNN each layer representations,

$$\min_{\mathcal{G}'} \mathbb{E}_{\Theta \sim \mathcal{P}_\Theta} \left[\sum_{t=1}^T D(\text{GNN}_{\Theta}(A', X'), \text{GNN}_{\Theta}(A, X)) \right]$$

where T is the number of GNN layers. GCDM has lower complexity than GCond, which only needs to calculate the distance between the distributions of the original graph and the synthetic graph, while GCond needs to calculate gradients and update the model parameters in each iteration, which is more expensive. GCDM doesn't fully utilize label information and still needs alternative training on GNN parameter and synthetic graph, resulting in limited performance.

Trajectory matching. SFSG [59] optimizes the synthetic graph by minimizing the difference between the trajectories of GNNs on original and synthetic graphs.

$$\min_{\mathcal{G}'} \mathbb{E}_{\Theta_{t,i}^* \sim \mathcal{P}_{\Theta_{t,i}^*}} \left[\mathcal{L}_{meta-tt}(\Theta_{t,i}^*|_{t=t_0}^p, \tilde{\Theta}_{t,i}^q|_{t=t_0}) \right]$$

$$s.t. \quad \tilde{\Theta}_{\mathcal{G}'}^* = \arg \min_{\Theta} \mathcal{L}(\text{GNN}_{\Theta}(A', X'), Y')$$

where $\Theta_{t,i}^*|_{t=t_0}^p$ are the parameters of GNN on \mathcal{G} in the training interval $[\Theta_{t_0,i}^*, \Theta_{t_0+p,i}^*]$ and $\tilde{\Theta}_{t,i}^q|_{t=t_0}$ are the parameters of GNN on \mathcal{G}' in the training interval $[\tilde{\Theta}_{t_0,i}^q, \tilde{\Theta}_{t_0+q,i}^q]$. Training experts to obtain trajectories is time-consuming, and experts may occupy a large amount of memory.

Eigen matching. GDEM [32] firstly conducts *singular value decomposition* (SVD) to the original adjacency matrix A to get eigen values $\Lambda \in \mathbb{R}^K$ and eigen-basis $U \in \mathbb{R}^{N \times K}$. Then GDEM aims to synthetic X', Y' and the synthetic eigen-basis U' , which can be formalized as below,

$$\min_{\mathcal{G}'} \sum_{k=1}^K D((X^\top U_k)(X^\top U_k)^\top, (X'^\top U'_k)(X'^\top U'_k)^\top) + D(U' U'^\top, I)$$

$$+ D' \left(Y^\top A X, Y'^\top \sum_{k=1}^K (1 - \Lambda_k) U'_k U_k'^\top X' \right)$$

The primary computational cost of GDEM lies in the SVD decomposition. As the size of the graph increases, the time required for

SVD decomposition grows rapidly, far exceeding the time needed for the matching process.

Performance matching. GC-SNTK [44] matches the performance of models on original and synthetic graphs by *kernel ridge regression* (KRR), which obtains the closed-form solution without bi-level optimization process. It can be written as:

$$\min_{\mathcal{G}'} \mathcal{L}_{pm} = \frac{1}{2} \|\mathcal{K}_{\mathcal{G}\mathcal{G}'}(\mathcal{K}_{\mathcal{G}'\mathcal{G}'} + \epsilon I)^{-1} Y' - Y\|_F^2$$

where $\mathcal{K}_{\mathcal{G}\mathcal{G}'} \in \mathbb{R}^{N \times n}$ and $\mathcal{K}_{\mathcal{G}'\mathcal{G}'} \in \mathbb{R}^{n \times n}$ are two graph kernels, which can be obtained by iterative aggregation on the graph. The high computational and space demands of KRR for graph data mainly stem from the quadratic cost of computing graph kernels, the quadratic storage requirement for the kernel matrix, and the cubic computation needed to invert it, making KRR challenging for large-scale graph datasets.

Training free. CGC [14] is a recently proposed method for fast and high quality graph condensation. It utilizes SGC feature propagation to get node embedding, and uses multi-layer embedding combination for label prediction via MSE.

$$\arg \min_{\mathbf{W}} \left\| \frac{1}{K} \sum_{k=1}^K \tilde{A}^k X W - Y \right\|_2^2$$

which has a closed form solution of \mathbf{W} : $\hat{\mathbf{W}} = (\frac{1}{T} \sum_{t=1}^T \tilde{A}^t X)^\dagger Y$

CGC doing clustering on the class-partitioned embedding H to get class-wise aggregation $R^{(y)}$, then synthetic the condensed node embedding by $H'^{(y)} = R^{(y)} H^{(y)}$. Through on condensed embedding similarity, the condensed adjacency matrix A' can be obtained. Finally, the synthetic node attribute X' follows:

$$\arg \min_{X'} \mathcal{L} = \|\tilde{A}^T X' - Y\|_2^2 + \alpha \text{tr}(X'^\top L' X')$$

which has the closed-form solution:

$$X' = ((\tilde{A}^T)^\top \tilde{A}^T + \alpha L')^{-1} (\tilde{A}^T)^\top H'$$

A notable similarity between our ClustGDD and CGC is that they both employ clustering to generate node attributes efficiently. However, compared to CGC, our ClustGDD has some advantages. In terms of motivation, we choose clustering because we have discovered the inherent theoretical connection between clustering and FID, an indicator for measuring the quality of synthetic graphs, which is different from the starting point of CGC. In terms of specific implementation, there are several key differences. First, CGC incorporates SGC propagation, which might miss some local information on large graph. Our method, on the other hand, uses the closed-form solution of GLS on the graph to balance local and global information, leading to better node attributes. Second, to address the issue of heterophilic over-smoothing from clustering, we refine the synthetic node attributes quickly and effectively. While our method sacrifices some speed within an acceptable range, the trade-off is well worth it, as we maintain a higher level of effectiveness.

Table 6: Hyperparameters of ClustGDD

Dataset	Ratio	T	α	E_1	β	ρ	T'	E_3	γ	λ	dropout	H
Cora	1.3%	5	0.8	80	0.01	0.06	2	2000	7.0	0.1	0.6	256
	2.6%	5	0.8	80	0.01	0.4	2	2000	7.0	0.1	0.6	256
	5.2%	20	0.8	80	0.01	0.4	2	2000	7.0	0.1	0.6	256
Citeseer	0.9%	2	0.8	120	0.01	0.06	1	80	6.0	0.1	0.7	256
	1.80%	2	0.5	120	0.01	0.21	1	200	0.3	0.1	0.8	128
	3.60%	2	0.5	120	0.01	0.2	1	200	5.4	0.1	0.7	256
arXiv	0.05%	20	0.92	1000	1.4	0.1	10	1000	0.5	0.1	0.6	256
	0.25%	18	0.91	1000	1.9	0.1	10	1000	1.0	0.1	0.6	256
	0.50%	20	0.92	1000	1.0	0.1	10	1000	1.0	0.1	0.6	256
Flickr	0.10%	2	0.8	2000	0.2	0.5	2	2000	5.6	0.8	0.6	256
	0.50%	2	0.8	2000	0.2	0.5	1	2000	5.6	1.0	0.6	256
	1.00%	2	0.8	2000	0.2	0.5	2	2000	5.6	0.8	0.6	256
Reddit	0.05%	10	0.92	800	3.5	0.1	7	600	1.6	0.015	0.6	512
	0.10%	10	0.92	800	3.3	0.1	7	600	1.0	0.015	0.6	512
	0.50%	20	0.95	800	0.8	0.1	10	1000	2.1	0.01	0.6	256

B Time Complexity Analysis of Graph Distillation Methods

We here calculate some graph distillation methods for comparison. For GCond[25], let T is the number of GNN layers, and r is the number of sampled neighbors per node. Denote the outer-loop be L_o and inner loop as L_i , the training epoch be E . The total complexity of GCond is $O(EL_oL_i r^T Nd^2 + EL_oL_i n^2 d^2)$.

For SFGC, let the product of the number of experts L_n and the training epochs of experts E , and the number of outer-loop L_o and the inner loop be L_i . The total complexity is $O(EL_n MdT + EL_n Nd^2 T + L_o L_i nd^2 T)$.

For GCSR, denote the number of experts as L_n , the training epochs of experts as E_t , the number of meta matching L_o and GNNs training epochs be E_i , the total complexity is $O(E_t L_n r^T Nd^2 + E_i L_o nd^2 T + n^3)$.

For GDEM, let the eigen basis number be N_k , the eigen-basis matching training epoch is E , the time complexity of GDEM can be written as $O(N_k N^2 + N_k Nd + Md + N_k En^2 + N_k Ed^2)$.

To simplify, we abbreviate L_n , L_t , L_o and L_i as L , and E , E_t , E_i as E . ClustGDD has better time complexity in terms of polynomial order ($O(ENnd + n^2 d + Md + M \log M)$). Compared to GCond, SFGC, GCSR, and GDEM, the complexity terms of ClustGDD do not include higher-order terms such as EL , L^2 or $N_k N^2$, which can lead to significantly higher computational costs as the scale of the data increases. Therefore, ClustGDD outperforms other algorithms in terms of efficiency when dealing with large-scale graph data, especially when N and d are large.

C Datasets and Implementations Details

C.1 Dataset Deatils

Cora. [40] is a citation network consisting of 2,708 papers with 5,429 citation links, where nodes represent papers and edges for citations. The node attributes are 1433-dimensional vectors obtained by using the bag-of-words representation of the abstract. It has 7 categories of different paper topics. Cora has a training set of 140 nodes (5.2%), a validation set of 500 nodes (18.5%), and a test set of 1,000 nodes (36.9%) for transductive node classification, with the remaining nodes typically used for unsupervised or semi-supervised learning.

Citeseer. [40] is another citation network. Similar to Cora, it contains papers and citations of computer science, with 3,327 nodes and

4,732 edges. It has 3,703-dimensional attributes and 6 topic classes. Citeseer includes a training set of 120 nodes (3.6%), a validation set of 500 nodes (15.0%), and a test set of 1,000 nodes (30.0%) for transductive node classification.

arXiv. [21] is from the Open Graph Benchmark (OGB). It includes 169,343 arXiv papers divided into 40 subjects, and 1,166,243 citations. It has 128-dimensional Word2Vec node attributes. The arXiv dataset is for transductive node classification with temporally splits. Its training set consisting of papers published up to 2017 (90,941 nodes, 53.7%), the validation set consisting of papers in 2018 (29,799 nodes, 17.6%), and the test set including papers from 2019 (48,603 nodes, 28.7%), emphasizing temporal generalization.

Flickr. [57] is a social network consisting of 89,250 users and 899,75 6 interactions. In this network, nodes stand for users, edges indicate follower relationships, and the node attributes are 500-dimensional visual features extracted from the images uploaded by users. The nodes can be categorized into 7 classes. Flickr is randomly split into a training set of 44,625 nodes (50%), a validation set of 22,312 nodes (25%), and a test set of 22,313 nodes (25%), used for evaluating inductive node classification task.

Reddit. [18] is another social network, with 232,965 users and 11,606,919 interactions. The users are grouped into 41 subReddit categories. User activity and text are represented by 602-dimensional node attributes. The Reddit dataset is also randomly divided, with a training set of 152,410 nodes (65.4%), a validation set of 23,699 nodes (10.2%), and a test set of 55,334 nodes (23.7%), designed for large-scale inductive node classification tasks.

C.2 Implementation Details

We implement the GNN models and graph distillation by PyTorch Geometric. We collect graphs Cora, Citeseer, arXiv, Flickr and Reddit from GCond. We obtain the synthetic graphs generated by GCond³, SFGC⁴, GCSR⁵, and GDEM⁶. Main experiments are conducted on a

³<https://github.com/ChandlerBang/GCond>

⁴<https://github.com/Amanda-Zheng/SFGC>

⁵<https://github.com/zclzcl0223/GCSR>

⁶<https://github.com/liuyang-tian/GDEM>

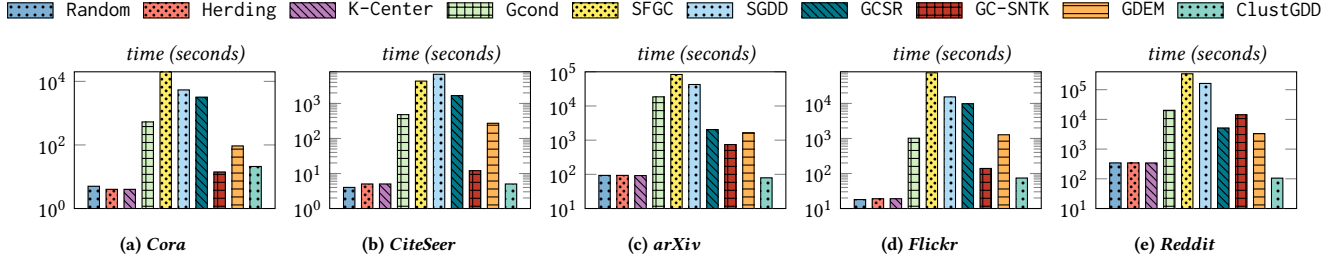


Figure 6: Computational time comparison

Linux machine equipped with an Intel(R) Xeon(R) Gold 6226 CPU @ 2.70GHz and a 32 GB Nvidia Tesla V100 GPU.

We set learning rate of GNNs to 0.01, the weight decay is $5e-4$. For ease of training, W and W' are two three-layer linear layers, with the middle layer having a dimension of H is in $\{128, 256, 512\}$. The dropout is in $\{0.6, 0.7, 0.8\}$.

We implement K-Means based on the Sklearn, the default maximum number of iterations E_2 for the K-means algorithm is 300. The algorithm will stop iterating if it converges earlier, meaning the change in cluster centers falls below the specified tolerance threshold, which is set to $1e-4$ by default. For large datasets *arXiv* and *Reddit*, we use Mini-Batch K-Means as an alternative, the batch size is set to 1000.

In the distillation stage, we conduct an extensive search to identify the optimal hyper-parameters. Specifically, we explore the following ranges for each hyper-parameter: the propagation times of the closed-form solution of GLS in clustering T are set to $\{2, 5, 10, 15, 18, 20, 25\}$; the coefficient in the propagation α is varied across $\{0.5, 0.8, 0.9, 0.91, 0.92, 0.95, 0.98\}$; the number of pretraining epochs E_1 is tested with values in $\{80, 100, 120, 800, 1000, 2000\}$; the combination weight of the refinement vector β is adjusted within the range $[0, 4]$; the propagation times in the refinement stage T' are set to $\{1, 2, 5, 7, 10\}$; the sampling rate in multi-view sparsification ρ is varied within the range $[0, 0.5]$; the number of refinement epochs E_2 is tested with values in $\{80, 100, 120, 800, 1000, 2000\}$; the weight of the supervision loss on the multi-view condensed graphs γ is adjusted within the range $[0, 10]$ and the weight of the consistency loss λ is adjusted within the range $[0, 1]$. This comprehensive search strategy allow us to fine-tune the model’s performance by systematically evaluating the impact of each hyper-parameter on the overall results. We record the hyper-parameters in Table 6.

For the evaluation stage, the evaluation model is set to GCN by default, which has two layers with 256 hidden dimensions, and dropout= 0.5, learning rate= 0.01, weight decay= $1e-5$, the training epochs is 600. In the generalization test, other GNN models have the same hidden dimensions, number of layers, learning rate, and dropout as GCN.

D Additional Experiments

D.1 Detailed Dataset Synthesis Time

In Fig. 6, we display the time costs required for GDD by ClustGDD and the other four competitive baselines (i.e., Gcond, SFGC, GCSR, and GDEM) on all five datasets with a condensation ratio of 2.6%, 1.8%, 0.05%, 0.10%, and 0.10%, respectively. The results for other condensation ratios are quantitatively similar and thus are omitted. The x-axis corresponds to different GDD methods, while the

y-axis represents the condensation time in seconds (s) in a logarithmic scale. As shown in Fig. 6, the computational time needed by ClustGDD is significantly (often orders of magnitude) less than those by the competitors on all datasets. For example, on *CiteSeer*, ClustGDD takes about 5s, which stands in stark contrast to the 479s needed by Gcond and 4334s for SFGC. On the *arXiv* dataset, the running time of ClustGDD is around 79s, while the others are up to more than 10,000 seconds.

Table 7: Statistics of original and condensed datasets.

Cora	Original	GCond	GCSR	ClustGDD
Nodes	2,708	70	70	70
Edges	5,429	4830	4900	1384
Avg Degree	2.00	69.0	70.0	19.77
Weighted Homophily	0.81	0.53	0.94	0.77
Storage(MB)	14.90	0.40	0.40	0.40
arXiv	Original	GCond	GCSR	ClustGDD
Nodes	169,343	90	90	90
Edges	1,166,243	8010	8084	5384
Avg Degree	6.89	89.00	89.82	59.82
Weighted Homophily	0.65	0.08	0.08	0.58
Storage(MB)	100.40	0.08	0.08	0.08
Reddit	Original	GCond	GCSR	ClustGDD
Nodes	232,965	153	153	153
Edges	57,307,946	9,190	23,409	18,093
Avg Degree	245.99	60.07	153.00	118.25
Weighted Homophily	0.78	0.10	0.21	0.65
Storage(MB)	435.50	0.44	0.44	0.44

D.2 Statistics of the Synthetic Graphs

As shown in Table 7, we compare some statistics of the original datasets and synthetic graphs obtained by different graph distillation methods, GCond, GCSR, and ClustGDD, including the number of nodes, edges, average degree, weighted homophily, and the memory required for storage. It should be noted that both GCond and GCSR provide synthetic graphs that have not been sparsified. These methods significantly reduce the number of nodes and edges, thereby decreasing storage requirements. For larger datasets, such as *arXiv* and *Reddit*, the reduction in storage is particularly noticeable. We also compare the weighted homophily of different graphs, which is the ratio of the sum of the weights of all edges between same

class nodes to the sum of the weights of all edges. We find that ClustGDD is closer to the weighted homophily of the original graph than GCond and GCSR, reflecting that our synthetic graph retains key information about the topology of the original graph.

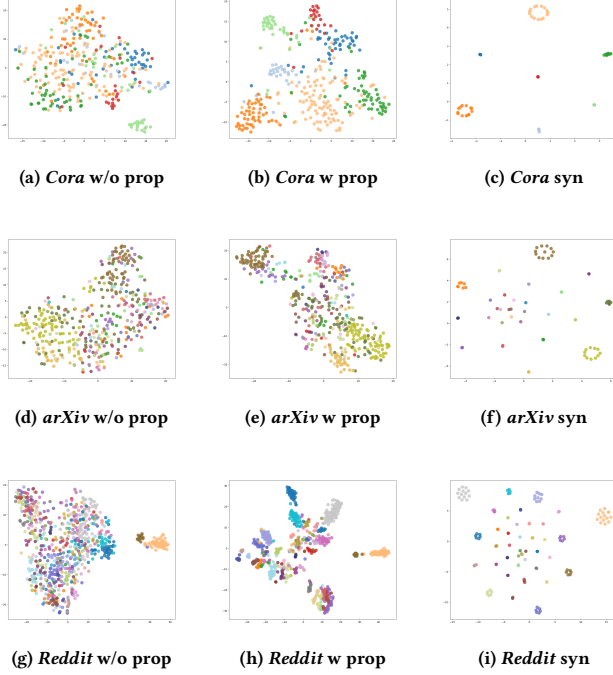


Figure 7: The visualization of prediction logits on non-propagated/propagated/synthetic attributes

D.3 Visualization

Propagation and Clustering. We first employ the T-SNE algorithm to visualize the logits of node attributes that have and have not undergone propagation after passing through a linear layer during the pretraining phase, as well as the logits of the synthetic node attributes after being processed by the GCN. As shown in Fig. 7, scatters of different colors represent nodes from different categories. We can clearly observe that the logits obtained from attributes processed by propagation exhibit much clearer classification boundaries compared to those that have not undergone propagation processing. Regarding the logits from the GCN on the synthetic graph, although they are fewer in number, they display the clearest classification boundaries and also exhibit diversity within the classes. This reflects the high quality of the synthetic nodes attributes.

Synthetic Graph Visualization. Next, we visualize the synthetic subgraph in Fig. 8. We choose to visualize edges with weights above a certain threshold, with the color of the edges becoming darker as the weight increases. We find that the intra-class and inter-class connections of nodes in the synthetic subgraph reflect the homophily

of the original graph, while the density of these connections indicates the density of the original graph. This demonstrates that our method has successfully synthetic informative graph data.

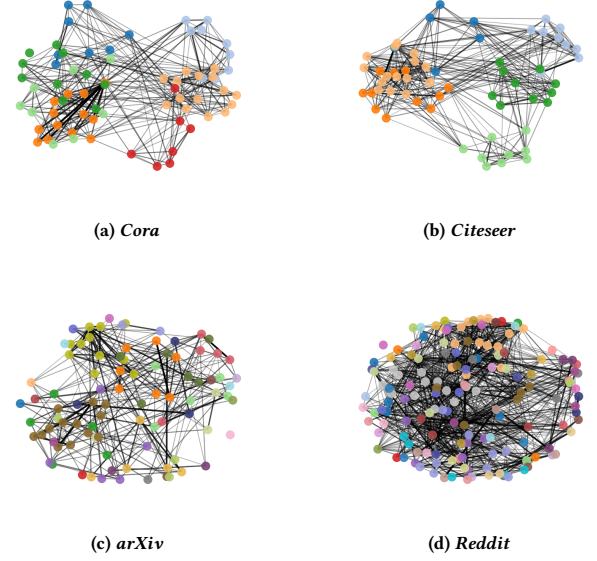


Figure 8: The visualization synthetic graphs

E Theoretical Proofs

Proof of Lemma 3.1. Using the Cauchy–Schwarz inequality, we can get

$$\begin{aligned}
 \|\mu^{\text{org}} - \mu^{\text{syn}}\|_2^2 &= \left\| \frac{1}{N} \sum_{v_j \in \mathcal{G}} H_j - \frac{1}{n} \sum_{u_i \in \mathcal{G}'} H'_i \right\|_2^2 \\
 &= \left\| \frac{1}{N} \sum_{i=1}^n \sum_{v_j \in C_i} H_j - \frac{1}{n} \sum_{u_i \in \mathcal{G}'} H'_i \right\|_2^2 = \left\| \sum_{i=1}^n \left(\frac{H'_i}{n} - \sum_{v_j \in C_i} \frac{H_j}{N} \right) \right\|_2^2 \\
 &= \left\| \sum_{i=1}^n \frac{1}{n} \cdot \left(H'_i - \sum_{v_j \in C_i} \frac{n}{N} \cdot H_j \right) \right\|_2^2 \leq \frac{1}{n} \sum_{i=1}^n \left\| H'_i - \sum_{v_j \in C_i} \frac{n}{N} \cdot H_j \right\|_2^2 \\
 &= \frac{1}{n} \sum_{i=1}^n \left\| \sum_{v_j \in C_i} \left(\frac{1}{|C_i|} - \frac{n}{N} \right) \cdot H_j \right\|_2^2.
 \end{aligned}$$

Since the Euclidean norm $\|\cdot\|_2^2$ is a convex function, using Jensen’s Inequality leads to

$$\begin{aligned}
 \frac{1}{n} \sum_{i=1}^n \left\| \sum_{v_j \in C_i} \left(\frac{1}{|C_i|} - \frac{n}{N} \right) H_j \right\|_2^2 &\leq \frac{1}{n} \sum_{i=1}^n \sum_{v_j \in C_i} \left(\frac{1}{|C_i|} - \frac{n}{N} \right)^2 \|H_j\|_2^2 \\
 &= \frac{1}{n} \sum_{i=1}^n \sum_{v_j \in C_i} \left(\frac{1}{|C_i|} - \frac{n}{N} \right)^2 \\
 &= \sum_{i=1}^n \left(\frac{1}{n} - \frac{|C_i|}{N} \right)^2 = \frac{1}{N^2} \sum_{i=1}^n \left(\frac{N}{n} - |C_i| \right)^2.
 \end{aligned}$$

The lemma is proved. \square

Proof of Lemma 3.2. First, according to the definitions in Eq. (4), Σ^{org} and Σ^{syn} are symmetric and positive semi-definite. By their positive semi-definiteness and Araki–Lieb–Thirring inequality [1], we have the following upper bound:

$$\begin{aligned} & \text{Tr}(\Sigma^{\text{org}}) + \text{Tr}(\Sigma^{\text{syn}}) - 2 \text{Tr}((\Sigma^{\text{org}} \Sigma^{\text{syn}})^{\frac{1}{2}}) \\ & \leq \text{Tr}(\Sigma^{\text{org}}) + \text{Tr}(\Sigma^{\text{syn}}) - 2 \text{Tr}(\Sigma^{\text{org} \frac{1}{2}} \Sigma^{\text{syn} \frac{1}{2}}) \\ & = \text{Tr}((\Sigma^{\text{org} \frac{1}{2}} - \Sigma^{\text{syn} \frac{1}{2}})^2) = \|\Sigma^{\text{org} \frac{1}{2}} - \Sigma^{\text{syn} \frac{1}{2}}\|_F^2 \\ & \leq \|\Sigma^{\text{org} \frac{1}{2}}\|_F^2 + \|\Sigma^{\text{syn} \frac{1}{2}}\|_F^2 = \text{Tr}(\Sigma^{\text{org}}) + \text{Tr}(\Sigma^{\text{syn}}). \end{aligned} \quad (19)$$

Next, we need the following two lemmata.

LEMMA E.1. *The following equation holds:*

$$\text{Tr}(\Sigma^{\text{org}}) = \frac{1}{N} \sum_{i=1}^n \sum_{v_j \in C_i} \|H_j - H'_i\|_2^2 + \sum_{i=1}^n \frac{|C_i|}{N} \|H'_i - \mu^{\text{org}}\|_2^2 \quad (20)$$

LEMMA E.2. $\sum_{i=1}^n \|H'_i - \mu^{\text{org}}\|_2^2 = n \cdot (\text{Tr}(\Sigma^{\text{syn}}) + \|\mu^{\text{syn}} - \mu^{\text{org}}\|_2^2)$

Combining Lemmata E.1, E.2, and Eq. (19) leads to

$$\begin{aligned} & \text{Tr}(\Sigma^{\text{org}}) + \text{Tr}(\Sigma^{\text{syn}}) \\ & = \frac{1}{N} \sum_{i=1}^n \sum_{v_j \in C_i} \|H_j - H'_i\|_2^2 + \sum_{i=1}^n \frac{|C_i|}{N} \|H'_i - \mu^{\text{org}}\|_2^2 + \text{Tr}(\Sigma^{\text{syn}}) \\ & = \frac{1}{N} \sum_{i=1}^n \sum_{v_j \in C_i} \|H_j - H'_i\|_2^2 + \frac{c_{\max}}{N} \sum_{i=1}^n \|H'_i - \mu^{\text{org}}\|_2^2 + \text{Tr}(\Sigma^{\text{syn}}) \\ & = \frac{1}{N} \sum_{i=1}^n \sum_{v_j \in C_i} \|H_j - H'_i\|_2^2 + \left(\frac{nc_{\max}}{N} + 1\right) \cdot \text{Tr}(\Sigma^{\text{syn}}) \\ & \quad + \frac{nc_{\max}}{N} \cdot \|\mu^{\text{syn}} - \mu^{\text{org}}\|_2^2. \end{aligned} \quad (21)$$

From Lemma E.2, we can further derive that

$$\begin{aligned} \text{Tr}(\Sigma^{\text{syn}}) & \leq \frac{1}{n} \sum_{i=1}^n \|H'_i - \mu^{\text{org}}\|_2^2 \leq \frac{1}{n} \cdot \frac{N}{c_{\min}} \sum_{i=1}^n \frac{|C_i|}{N} \|H'_i - \mu^{\text{org}}\|_2^2 \\ & \leq \frac{N}{nc_{\min}} \cdot \text{Tr}(\Sigma^{\text{org}}). \end{aligned}$$

Plugging the above inequality into Eq. (21) finishes the proof. \square

Proof of Lemma E.1. Recall that $\Sigma_{a,b}^{\text{org}}$ represents the covariance between the dimension a and dimension b of H . Then,

$$\Sigma_{a,b}^{\text{org}} = \frac{1}{N} \sum_{v_j \in \mathcal{G}} (H_{j,a} - \mu_a^{\text{org}})(H_{j,b} - \mu_b^{\text{org}}) \quad (22)$$

where $\mu_a^{\text{org}}, \mu_b^{\text{org}}$ are the means of dimension a and b respectively. The covariance matrix can be decomposed into an intra-cluster covariance matrix and an inter-cluster covariance matrix. Note that we have

$$\begin{aligned} H_{j,a} &= H'_{i,a} + (H_{j,a} - H'_{i,a}), \\ H_{j,b} &= H'_{i,b} + (H_{j,b} - H'_{i,b}), \\ \sum_{v_j \in C_i} (H_{j,a} - H'_{i,a}) &= \sum_{v_j \in C_i} (H_{j,b} - H'_{i,b}) = 0. \end{aligned}$$

Then $\Sigma_{a,b}^{\text{org}}$ can be rewritten as:

$$\begin{aligned} \Sigma_{a,b}^{\text{org}} &= \frac{1}{N} \sum_{i=1}^n \sum_{v_j \in C_i} ((H_{j,a} - H'_{i,a}) + (H'_{i,a} - \mu_a^{\text{org}})) \\ & \quad \cdot ((H_{j,b} - H'_{i,b}) + (H'_{i,b} - \mu_b^{\text{org}})) \\ &= \sum_{i=1}^n \frac{|C_i|}{N} \cdot (H'_{i,a} - \mu_a^{\text{org}})(H'_{i,b} - \mu_b^{\text{org}}) \\ & \quad + \frac{1}{N} \sum_{i=1}^n \sum_{v_j \in C_i} (H_{j,a} - H'_{i,a})(H_{j,b} - H'_{i,b}) \\ & \quad + \frac{1}{N} \sum_{i=1}^n \sum_{v_j \in C_i} (H_{j,a} - H'_{i,a})(H'_{i,b} - \mu_b^{\text{org}}) \\ & \quad + \frac{1}{N} \sum_{i=1}^n \sum_{v_j \in C_i} (H_{j,b} - H'_{i,b})(H'_{i,a} - \mu_a^{\text{org}}) \\ \Sigma_{a,b}^{\text{org}} &= \sum_{i=1}^n \frac{|C_i|}{N} \cdot (H'_{i,a} - \mu_a^{\text{org}})(H'_{i,b} - \mu_b^{\text{org}}) \\ & \quad + \frac{1}{N} \sum_{i=1}^n \sum_{v_j \in C_i} (H_{j,a} - H'_{i,a})(H_{j,b} - H'_{i,b}) \end{aligned} \quad (23)$$

According to Eq. (23),

$$\text{Tr}(\Sigma^{\text{org}}) = \frac{1}{N} \sum_{i=1}^n \sum_{v_j \in C_i} \|H_j - H'_i\|_2^2 + \sum_{i=1}^n \frac{|C_i|}{N} \|H'_i - \mu^{\text{org}}\|_2^2,$$

which completes the proof. \square

Proof of Lemma E.2. According to Eq. (3), $\sum_{i=1}^n \|H'_i - \mu^{\text{org}}\|_2^2$ can be expanded as

$$\sum_{i=1}^n \|H'_i - \mu^{\text{org}}\|_2^2 = \sum_{i=1}^n (H'_i - \mu^{\text{org}})^\top (H'_i - \mu^{\text{org}}).$$

Let $\Delta = \mu^{\text{org}} - \mu^{\text{syn}}$, we have

$$\begin{aligned} & \sum_{i=1}^n (H'_i - \mu^{\text{org}})^\top (H'_i - \mu^{\text{org}}) \\ &= \sum_{i=1}^n (H'_i - \mu^{\text{syn}} + \Delta)^\top (H'_i - \mu^{\text{syn}} + \Delta) \\ &= \sum_{i=1}^n ((H'_i - \mu^{\text{syn}})^\top (H'_i - \mu^{\text{syn}}) + 2(H'_i - \mu^{\text{syn}})^\top \Delta + \Delta^\top \Delta) \end{aligned}$$

Since $\sum_{i=1}^n (H'_i - \mu^{\text{syn}}) = 0$, we have

$$\begin{aligned} \sum_{i=1}^n \|H'_i - \mu^{\text{org}}\|_2^2 &= \sum_{i=1}^n (\|H'_i - \mu^{\text{syn}}\|_2^2 + \|\mu^{\text{syn}} - \mu^{\text{org}}\|_2^2) \\ &= n \cdot (\text{Tr}(\Sigma^{\text{syn}}) + \|\mu^{\text{syn}} - \mu^{\text{org}}\|_2^2). \end{aligned}$$

The lemma then follows. \square

Proof of Lemma 4.1. First, the second term is equivalent to

$$\sum_{(v_i, v_j) \in \mathcal{E}} \left\| \frac{H_i}{\sqrt{d(v_i)}} - \frac{H_j}{\sqrt{d(v_j)}} \right\|_F^2 = \text{Tr}(H^\top (I - \tilde{A})H).$$

By setting its derivative w.r.t. H to zero, we obtain the optimal H as:

$$\begin{aligned} \frac{\partial \{ (1 - \alpha) \cdot \|H - XW\|_F^2 + \alpha \cdot \text{Tr}(H^\top (I - \tilde{A})H) \}}{\partial H} &= 0 \\ \implies (1 - \alpha) \cdot (H - XW) + \alpha(I - \tilde{A})H &= 0 \\ \implies H &= (1 - \alpha) \cdot (I - \alpha\tilde{A})^{-1} XW. \end{aligned} \quad (24)$$

By the property of Neumann series, we have $(I - \alpha\tilde{A})^{-1} = \sum_{\ell=0}^{\infty} \alpha^\ell \tilde{A}^\ell$. Plugging it into Eq. (24) completes the proof. \square

Proof of Lemma 4.2. Recall that the definition of homophily ratio over graph \mathcal{G} is the fraction of edges whose endpoints are in

the same class. Thus,

$$\begin{aligned} \Omega(\mathcal{G}) &= \frac{\sum_{(v_i, v_j) \in \mathcal{E}} \sum_{k=1}^K Y_{i,k} \cdot Y_{j,k}}{m} \\ &= - \frac{\sum_{(v_i, v_j) \in \mathcal{E}} \sum_{k=1}^K Y_{i,k}^2 - Y_{i,k}^2 + Y_{j,k}^2 - Y_{j,k}^2 - 2Y_{i,k} \cdot Y_{j,k}}{2M} \\ &= \frac{\sum_{(v_i, v_j) \in \mathcal{E}} \sum_{k=1}^K Y_{i,k}^2 + Y_{j,k}^2}{2m} \\ &\quad - \frac{\sum_{(v_i, v_j) \in \mathcal{E}} \sum_{k=1}^K Y_{i,k}^2 + Y_{j,k}^2 - 2Y_{i,k} \cdot Y_{j,k}}{2M} \\ &= 1 - \frac{\sum_{(v_i, v_j) \in \mathcal{E}} \sum_{k=1}^K (Y_{i,k} - Y_{j,k})^2}{2m} \\ &= 1 - \frac{\sum_{(v_i, v_j) \in \mathcal{E}} \|Y_i - Y_j\|_2^2}{2M} \\ &= 1 - \frac{\sum_{(v_i, v_j) \in \mathcal{E}} \left\| \frac{(D^{1/2}Y)_i}{\sqrt{d_i}} - \frac{(D^{1/2}Y)_j}{\sqrt{d_j}} \right\|_2^2}{2M}, \end{aligned}$$

which finishes the proof. \square